

CONTENTS N THROUGH Z

Observational and Theoretical Constraints on the Initial Temperature Structures of the Terrestrial Planets <i>F. Nimmo</i>	4007
Melt-Solid Segregation, Fractional Magma Ocean Solidification, and Implications for Planetary Evolution <i>E. M. Parmentier, L. Elkins-Tanton, and P. C. Hess</i>	4044
Osmium Isotope Systematics of Ureilites <i>K. Rankenburg, A. D. Brandon, and M. Humayun</i>	4047
Comparative Planetary Differentiation: Siderophile Element Constraints on the Depth and Extent of Melting on Early Mars <i>K. Righter</i>	4041
Highly Siderophile Elements in the Terrestrial Upper Mantle Require a Late Veneer? New Results for Palladium <i>K. Righter, M. Humayun, and L. Danielson</i>	4040
Processing of the Earth's Upper Continental Crust by Impacts of Magmatic Iron Meteorites and/or Pallasites: Evidence from HSE and Ni? <i>G. H. Schmidt</i>	4027
Role of Proto-Cores in Terrestrial Planet Differentiation <i>H. H. Schmitt</i>	4054
Possible Core Formation Within Planetesimal Due to Permeable Flow <i>H. Senshu and T. Matsui</i>	4021
Remnants of a Magma Ocean. Insights into the Early Differentiation of the Moon and Its Relevance to the Differentiation of the Terrestrial Planets <i>C. K. Shearer</i>	4015
Exploring the Differentiation of the Terrestrial Planets Through Future Sample Return Missions to the Moon and Construction of a Lunar Geophysical Network <i>C. K. Shearer, C. Neal, L. Borg, and B. Jolliff</i>	4058
Early Planetary Differentiation: An Overview <i>D. J. Stevenson</i>	4059
^{176}Lu - ^{176}Hf in Lunar Zircons: Identification of an Early Enriched Reservoir on the Moon <i>D. J. Taylor, K. D. McKeegan, T. M. Harrison, and M. McCulloch</i>	4045
The Type Ia Supernova as a Key to Origin of the Solar System <i>G. K. Ustinova</i>	4002
Bulk Earth Compositional Models are Consistent with the Presence of Potassium in Earth's Core <i>W. van Westrenen and V. Rama Murthy</i>	4004
Osmium Isotope and Highly Siderophile Element Abundance Constraints on the Nature of the Late Accretionary Histories of the Earth, Moon and Mars <i>R. J. Walker</i>	4008

Exploring the Geochemical Consequences of Magma Ocean Differentiation <i>M. J. Walter</i>	4028
Siderophile Element Implications for the Style of Differentiation of the HED Parent Body <i>P. H. Warren</i>	4056
Earth After the Moon-forming Impact <i>K. J. Zahnle and W. B. Moore</i>	4039

OBSERVATIONAL AND THEORETICAL CONSTRAINTS ON THE INITIAL TEMPERATURE STRUCTURES OF THE TERRESTRIAL PLANETS. F. Nimmo, *Dept. Earth & Planetary Sciences, University of California Santa Cruz, Santa Cruz, CA 95064 (fnimmo@es.ucsc.edu).*

The initial temperature structure of a terrestrial planet is important for several reasons: it controls where and when melting (and iron-silicate differentiation) occurs; it controls the abundance and distribution of volatile species; and it will have a significant effect on the longer-term thermal evolution of the planet. Here I will discuss observational and theoretical constraints on how the accretion process controls the initial temperature structure, with reference to the Earth and Mars.

An evolving planet's temperature structure depends on the surface temperature, the manner in which heat is transported, and the energy sources available. Three energy sources are particularly relevant: energy delivered by impacts; energy from radiogenic isotopes; and energy released during core formation. All three of these energy sources depend strongly on the manner in which a planet accretes.

If accretion is sufficiently rapid, short-lived radiogenic isotopes result in high central temperatures and melting for even moderately-sized bodies. Partial melting is likely to result in core formation [1]. There is now strong evidence for such melting having occurred among certain classes of asteroids [2], suggesting that at least some of the embryos which built the terrestrial planets were already differentiated.

Core formation is favoured in partially molten systems, and results in a further release of gravitational energy [3]. Because of the likely rapid transit of iron diapirs, the result is cores which are substantially hotter than the overlying mantle.

The effects of impacts on planetary temperature structures are poorly understood. "Small" impacts deliver most of their heat in the near sub-surface and result in inverted temperature structures (planetary interiors are cold) [4]. "Giant" impacts conversely deliver heat at greater depths, and for Mars-sized and larger planets deliver an order of magnitude more energy than short-lived radiogenic species (Fig. 1). Oligarchic growth involves a mix of "small" and "giant" impacts, while the final stage of planetary accretion only involves the latter [5] (see Fig. 1). "Giant" impacts result in magma ponds or magma oceans [6], but the lifetime of these bodies is not well constrained. The presence of magma oceans permits rapid core formation [1].

The Earth is sufficiently large that wide-spread melting during the final stages of accretion was inevitable. Hf-W data on the core formation timescale (≈ 30 Myr) are consistent with numerical accretion calculations, assuming that re-equilibration of the impactor material with the mantle occurred [7]. Magma ocean conditions controlled the abundance of secondary elements in the core, and may be estimated from mantle siderophile element abundances [8]. Core formation resulted in a core at least several hundred K hotter than the overlying mantle, which probably melted [9].

Little is currently understood about the early temperature structure of Mars. Neither theoretical nor observational approaches have resolved whether or not Mars possessed an early

magma ocean [10]. Likewise, the timescale of core formation is uncertain ($\approx 1-10$ Myr) [11,12], but does suggest that Mars cannot have been built entirely from "small" impacts. An initially hot Martian core is consistent with the early existence of a dynamo [13].

References

- [1] Stevenson, D.J., in *Origin of the Earth*, OUP 1990.
- [2] Srinivasan, G. et al., *Science* 284, 1358-1360, 1999.
- [3] Solomon, S.C., *PEPI* 19, 168-182, 1979.
- [4] Kaula, W.M., *JGR* 84, 999-1008, 1979.
- [5] Agnor, C.B. et al., *Icarus* 142, 219-237, 1999.
- [6] Tonks, W.B. and H.J. Melosh, *JGR* 98, 5319-5333, 1993.
- [7] Nimmo, F. and C.B. Agnor, *EPSL* 243, 26-43, 2006.
- [8] Righter, K., *AREPS* 31, 135-174, 2003.
- [9] Nimmo, F., *Treatise on Geophysics*, submitted.
- [10] Halliday, A.N. et al., *Space Sci. Rev.* 96, 197-230, 2001
- [11] Jacobsen, S.B., *AREPS* 33, 531-570, 2005.
- [12] Kleine, T. et al., *GCA* 68, 2935-2946, 2004.
- [13] Williams, J.-P. and F. Nimmo, *Geology* 32, 97-100, 2004.

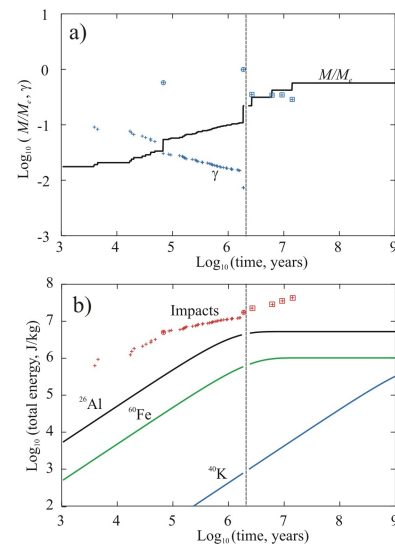


Figure 1: a) Schematic growth of a proto-Earth. Early growth is from Agnor (unpub.) where the initial mass distribution consists of 11 embryos and 900 non-interacting planetesimals. Late growth is from [5]. The vertical dashed line denotes the splicing time. The solid line shows the mass evolution of the body, and the crosses denote the target:impactor mass ratio γ . Circles denote embryo-embryo collisions; squares late-stage giant impacts. b) Corresponding energy production. The cumulative energy due to impacts (crosses) is calculated using equation (8) of [9] for each impact. Solid lines show the energy associated with radioactive elements.

MELT-SOLID SEGREGATION, FRACTIONAL MAGMA OCEAN SOLIDIFICATION, AND IMPLICATIONS FOR PLANETARY EVOLUTION. E.M. Parmentier, L. Elkins-Tanton, and P.C. Hess, Department of Geological Sciences, Brown University, Providence, RI, 02912 (EM.Parmentier@brown.edu).

Introduction: Large planetary bodies are likely to have been significantly melted during their accretion, simply as a consequence of the potential energy of accretion if accretion occurs rapidly enough or possibly due to giant impacts [1]. Since the solidus and liquidus temperatures of mantle mineral assemblages increase with pressure more rapidly than temperature along an adiabat, solidification of a thermally well-mixed magma ocean (MO) is expected to occur from the bottom up. If the surface temperature is below the liquidus, crystallization may also occur in the cool thermal boundary layer at the planetary surface.

Ideal fractional solidification of a MO results in an unstable stratigraphy primarily due to increasing Fe/Mg of residual liquid as solidification proceeds. Highly incompatible elements, including heat producing U, Th, and K, would be progressively enriched in the residual liquid. The unstable stratigraphy resulting from fractional solidification would overturn on relatively short time scales with significant implications resulting in a stably stratified mantle that would resist solid-state thermal convection and in which incompatible heat producing elements are concentrated at the bottom of the mantle with fundamental implications for long term planetary evolution [2,3,4].

Fractional solidification requires the separation of solid from the liquid in which it forms. The rate of this separation may thus control how ideally fractional the MO solidification can be. Cooling of the MO is expected to be controlled by the radiative cooling of the planetary surface, thus depending on the pressure and composition of the atmosphere [5,6]. The rapidity of early planetary evolution is indicated by the presence of significant fractionations in the daughter products of isotopic decay that must have occurred during the earliest evolution, including variation in ^{182}W [7] and ^{142}Nd [8,9] that are produced from decay with half-lives of approximately 10 and 100 Myr, respectively.

Solid-melt segregation during MO solidification: Crystallization will occur in cool sinking plumes and thermals that develop from instability of the surface thermal boundary layer and in the thermal boundary layer itself if the surface temperature is below the liquidus. Figure 1 illustrates the case with solidification occurring only in downwelling plumes. Due to turbulent entrainment the plume radius increases as about $0.1 \times \text{depth}$ [10,11]. Solids forming in the cool central region of the plume will impinge on the solidified floor of the MO and spread laterally to form a layer of solid containing interstitial melt with a melt fraction that increases upward. The top of this mostly

solid layer will occur at a height where the melt fraction reached about 50%, corresponding to fraction of the radius of the plume. For a MO depth of 500 km this layer should be about 100 km thick. Much like atmospheric convective upwelling resulting from heating of the earth's surface, cool turbulent plumes in a MO are expected to be highly time dependent. Deposition of partially molten material in layers beneath plumes will thus be episodic at an average deposition rate determined by the overall cooling at the surface. For an average solidification velocity V and a layer thickness H , the average time between depositions and the time for each layer to lose its melt before being buried beneath the next layer would be simply H/V .

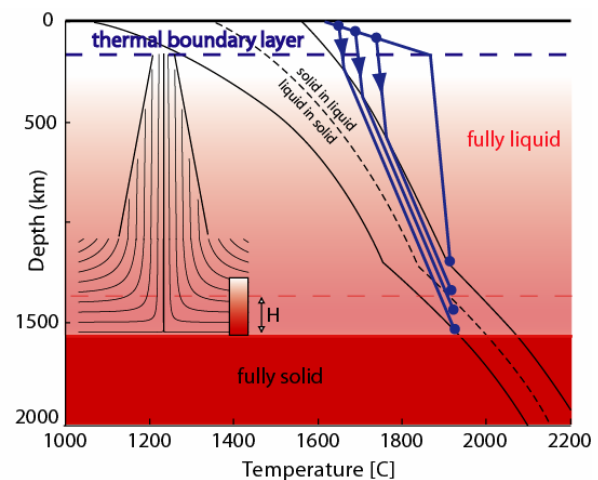


Figure 1. Temperature-pressure paths in a thermal plume emanating from the cold surface thermal boundary layer. Solidification by adiabatic compression. decreases from the plume center where temperatures are lowest. The plume widens with depth due to turbulent entrainment. Each plume deposits a layer of thickness H that thins radially away from the plume.

The migration of buoyant melt out of each layer will be controlled by porous flow of liquid through the solid, as described by a permeability K and liquid viscosity μ , and the compaction rate of the solid with a viscosity ζ , expected to be comparable to the shear viscosity of the solid deforming by thermally activated creep. Compaction resistance is important only on spatial scales comparable to the compaction length $(K\zeta/\mu)^{1/2}$ [12]. For intragranular flow with grain size b and melt fraction ϕ , $K = b^2 \phi^3 / 270$ [13]. For the typical values $b \sim 1\text{mm}$, $\phi \sim 1\%$, $\zeta \sim 10^{18}\text{Pa}\cdot\text{s}$, and $\mu = 10\text{Pa}\cdot\text{s}$, the compaction length $\sim 10\text{-}10^2\text{m}$ is relatively small compared to the 10-100 km layer thickness. The compaction resistance is thus expected to be small. The

vertical migration of melt with a volumetric flow rate S thus reflects a balance of pressure gradients due to percolation and buoyancy forces $\mu S/K = \Delta\rho g$, where $\Delta\rho$ is the solid-liquid density difference. The evolution of melt fraction with time t as a height z above the bottom of the layer is governed by the mass balance

$$\frac{\partial\phi}{\partial t} + \frac{dS}{d\phi} \frac{\partial\phi}{\partial z} = 0. \quad (1)$$

With $dS/d\phi = S^* \phi^{-2}$ and an initial distribution of ϕ increasing linearly with z , solutions of (1) are shown in Figure 2. Times on the order of $10 S^*/H$ and $1000 S^*/H$ are required to reduce the retained melt fraction to about 10% and 1%, respectively. For bulk solidification rate V , the time between the emplacement of successive layers is $\sim H/V$. Then based on the results of Figure 2, $S^*/V = 1000$ and 10 correspond to retained melt fractions averaged over depth z of approximately 1% and 10%, respectively.

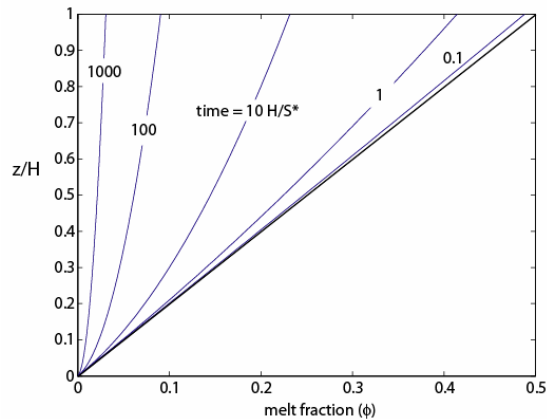


Figure 2. Melt fraction as a function of height in a layer of thickness H for an initial linear melt fraction distribution.

Implications of melt retention for fractional solidification: The radial density variation due to fractional solidification of a Mars-like planet with several different values of retained interstitial melt content is shown in Figure 3. With 10% retained melt the density instability is substantially reduced, but 1% retained melt approximates ideal fractional solidification. Incompatible elements are even more sensitive to retained melt fraction. A 1000 km deep MO may solidify in times ranging from 10^{-2} Myr to 10 Myr depending on the mass and composition of the atmosphere [5], corresponding to S^*/V values in the range of 0.3 to 300. Thus the amount of retained melt and its effect on solid-state planetary evolution may depend very significantly on the presence and composition of an early atmosphere. Solidification times on the order of 10 Myr as suggested by isotope systematics would be consistent with retained melt fractions of at most a few

percent. S^* also depends sensitively on b , so that the development of melt channels could significantly reduce the amount of retained melt.

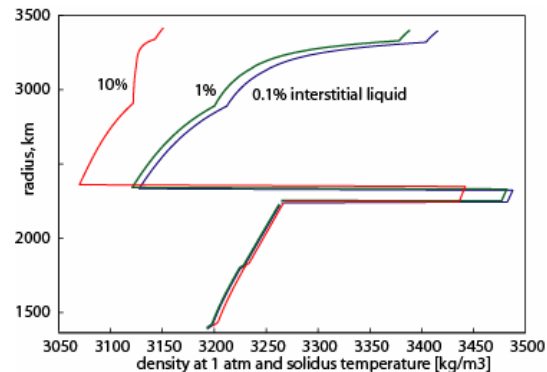


Figure 3. Density as a function of radius following fractional solidification with a range of retained interstitial melt volume fraction.

Turbulent suspension of solid mineral grains:

As cool sinking plumes spread radially at the top of the mostly solidified layer, solid mineral grains in the overlying mostly liquid layer that are denser than the liquid will settle. Flow in turbulent eddies will act to keep particles suspended thus reducing solid-liquid separation in the solidifying magma ocean. A simple estimate can be obtained by assuming that mineral grains are transported diffusively with the eddy diffusivity $K = 0.4 u^* y$ of shear driven turbulence. Here y is height above the top of the mostly solid layer and $u^* = (\tau/\rho)^{1/2}$ with shear stress τ . Mass balance also requires a region of upwelling surrounding the downwelling plume. The balance between this upwelling, gravitational settling of particles, and their turbulent diffusion determines the distribution of solid mineral grains. Since both the shear stress and upwelling decrease radially from the plume center, such an analysis does not indicate the perpetual suspension of solids during the solidification of a convecting MO.

References: [1] Melosh, H.J., in *Origin of the Earth*, Oxford U. Press, 69-83, 1990. [2] Elkins-Tanton, L., et al. (2005) *Earth Planet. Sci. Lett.* 236, 1-12. [3] Elkins-Tanton, L., et al. (2005) *J. Geophys. Res.* 110, doi:10.1029/2005-JE002480. [4] Blichert-Toft, J., et al. (1999) *Earth Planet. Sci. Lett.* 173, 25-39. [5] Abe Y. (1997) *Phys. Earth Planet. Int.* 100, 27-39. [6] Solomatov V.S. (2000) in *Origin of the Earth and Moon*, University of Arizona Press, 323-338. [7] Jacobsen, S.B. (2005) *Ann. Rev. Earth Planet. Sci.* 33 [8] Harper C.L. et al. (1995) *Science* 267, 213-217. [9] Borg L.E., et al. (1997) *Geochimica et Cosmochimica Acta* 61, 4915-4931. [10] Priestley, C.H.B. (1956) *Proc. Roy. Soc. London* A238, 287-304. [11] Morton, B.R., et al. (1956) *Proc. Roy. Soc. London* A234, 1-23. [12] Stevenson, D.J., and Scott., D.R. (1991) *Ann. Rev. Fluid Mech.* 23, 305-339. [13] Wark, D.A., et al. (2003.) *J. Geophys. Res.* 108, 1-13.

OSMIUM ISOTOPE SYSTEMATICS OF UREILITES. K. Rankenburg^{1,2}, A. D. Brandon² and M. Humayun¹.
¹NHMFL and Dept. of Geological Sciences, Florida State University, Tallahassee, FL 32310, USA. ²NASA JSC, Mail Code KR, Houston, TX 77058, USA, alan.d.brandon1@jsc.nasa.gov.

Introduction: The ureilites represent the second largest group among the achondritic meteorites comprising 16.2% of all achondrites. The prevailing two origins proposed for the ureilites are either as melting residues of carbonaceous chondritic material [1,2], or alternatively, derivation as mineral cumulates from such melts [35]; and both of these origins may be appropriate for different ureilites that have distinct compositional characteristics. However, ureilites are best known as enigmatic achondrites that preserve a substantial nebular signature in their oxygen isotope compositions that distinguishes them from other achondrite groups [6,7].

Recently, it has been shown that there are significant differences in the $^{187}\text{Re}/^{188}\text{Os}$ and $^{187}\text{Os}/^{188}\text{Os}$ ratios of carbonaceous chondrites compared with ordinary and enstatite chondrites [8]. Therefore, the Os isotopic compositions may prove useful for ‘fingerprinting’ the provenance of planetesimals. In order to better constrain the provenance of the ureilite protolith material and subsequent magmatic processing of the putative ureilite parent body (or bodies), the $^{187}\text{Os}/^{188}\text{Os}$ ratios for 22 ureilite whole rock samples, including monomict, augite-bearing, and polymict lithologies, were examined by N-TIMS. The Re-Os systematics are also explored in order to determine whether Re-Os chronology can provide constraints on the timing of ureilite differentiation.

Results: The Re and Os abundances for the studied ureilites range from ~0.1 times CI [8] in ALHA 81101 to ~2.6 times CI in ALHA 78019. The ureilite $^{187}\text{Os}/^{188}\text{Os}$ ratios form a unimodal distribution, and range from 0.11739 to 0.13018, with a mean of 0.1257 ± 0.0024 (1σ) (Fig. 1).

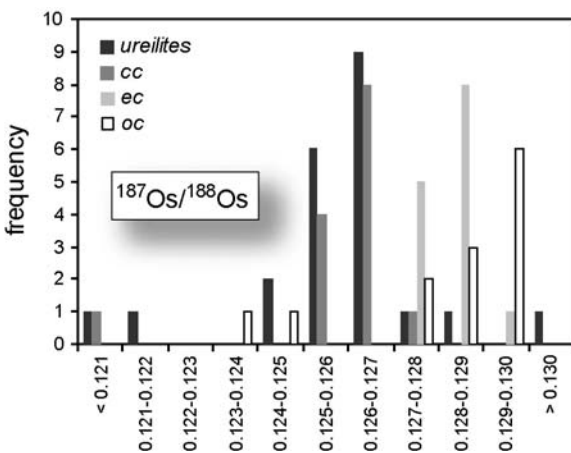


Fig. 1

There are no significant correlations of Os isotopic compositions with olivine or pyroxene core compositions, shock level, modal pyroxene content, $\delta^{33}\text{S}$, or $\Delta^{17}\text{O}$. The measured

$^{187}\text{Os}/^{188}\text{Os}$ ratios were used to infer time averaged $^{187}\text{Re}/^{188}\text{Os}$ ratios for the samples, assuming an age of the ureilites of 4562 Ma [9]. From these ratios, and the measured Os concentrations, average time-integrated Re concentrations were calculated for each ureilite and are compared with the measured Re concentrations (Fig. 2).

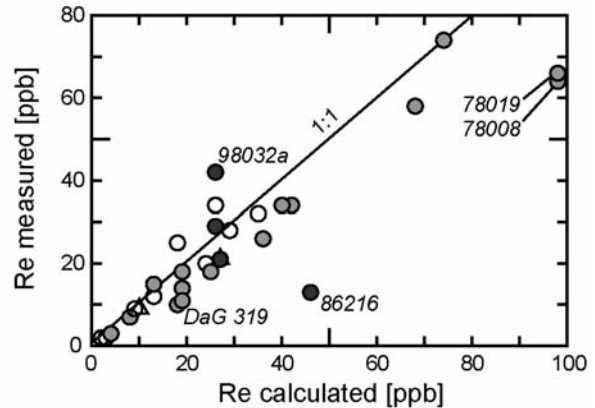


Fig. 2

The measured and calculated Re concentrations are correlated and scatter around a 1:1 reference line. Correlation coefficients are similarly high among groups of samples classified as weathering grades ‘A’ (minor rustiness – open symbols in Fig. 2) and ‘B’ (moderate rustiness – grey symbols) with $r^2 = 0.91$ and 0.94 , respectively. In contrast, samples classified as ‘C’ (severe rustiness – black symbols) show large scatter ($r^2 = 0.31$).

Because of the overall large scatter in Re/Os ratios, no meaningful age information can be deduced from the ureilite whole rock data. Even when the dataset is restricted to the group of ureilite falls (with apparently undisturbed Re-Os isotopes), no isochron can be fitted to the data because of the insufficient range in Re/Os ratios. However, a subset of the ureilite whole rock data including the falls cluster more closely around a 4562 Ma reference isochron (Fig. 3).

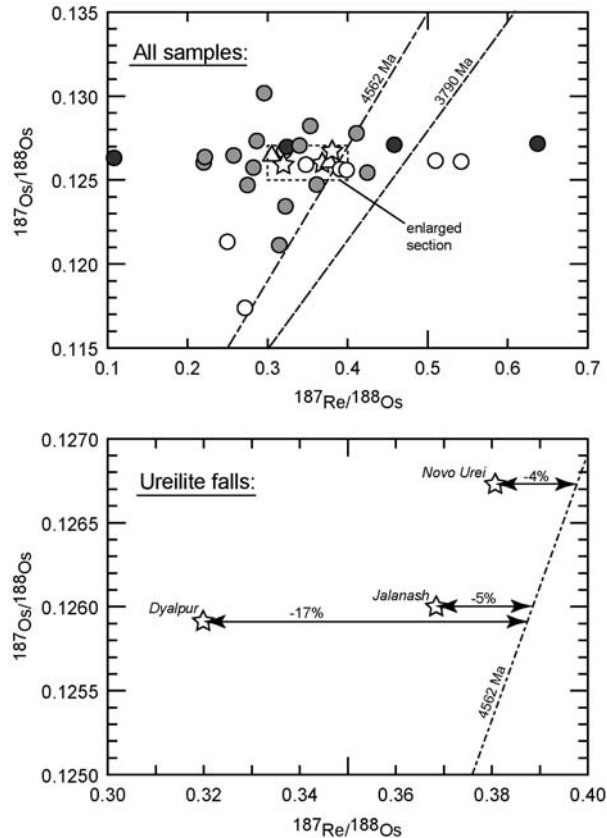


Fig. 3

The mean and distribution of $^{187}\text{Os}/^{188}\text{Os}$ isotope ratios measured in 22 ureilites (0.1257 ± 0.0024) are similar to those measured in carbonaceous chondrites (0.1258 ± 0.0018), but different to those measured for ordinary chondrites (0.1281 ± 0.0020) or enstatite chondrites (0.1281 ± 0.0005) [8]. The division of bulk chondrites based upon $^{187}\text{Os}/^{188}\text{Os}$ ratios into two groups (carbonaceous versus ordinary/enstatite chondrites) has been proposed to result most likely from high-temperature nebular condensation of refractory element-bearing alloys and their subsequent isolation and incorporation into the precursor materials of certain chondrite groups [8]. The ureilite $^{187}\text{Os}/^{188}\text{Os}$ average of 0.1257 ± 0.0024 (1σ) is identical within uncertainty to the average of carbonaceous chondrites, and distinct from ordinary or enstatite chondrites. The similar mean of $^{187}\text{Os}/^{188}\text{Os}$ ratios measured for the ureilites and carbonaceous chondrites suggests that the ureilite parent body probably formed from similar precursor material, i.e. probably within the same region of the solar nebula as carbonaceous chondrites. The polymict (brecciated) ureilites have been proposed to be representative of the complete ureilite parent body because the constituent minerals of each polymict ureilite encompass the compositional spectrum of the monomict ureilites as a whole [10,11]. Therefore, the $^{187}\text{Os}/^{188}\text{Os}$ ratio of 0.1262 ± 0.0004 (2σ) measured in this study for the polymict ureilite

DaG 319, which is indistinguishable from the average of the 22 monomict ureilites measured in this study, can be taken as an independent confirmation of the average $^{187}\text{Os}/^{188}\text{Os}$ ratio of the ureilite parent body as a whole.

Although the ureilites and carbonaceous chondrite groups are similar in respect to their Os (and oxygen) isotopic compositions, the ureilites are different from the carbonaceous chondrites in that they experienced magmatic processing, i.e. they were heated to a much larger degree. If radioactive decay of short-lived radionuclides such as ^{26}Al is a predominant heat source for early planetary differentiation, then the degree of magmatic processing in accreting planetary bodies is dependent on their size and their time of accretion [e.g. 12]. Ureilites therefore could represent a parent body that accreted earlier than the CC parent body (-ies), represent a parent body that accreted contemporaneously with CC but was large enough to allow for incipient melting, or simply represent the warmer interior of a larger CV-type carbonaceous chondrite parent body.

References:

- [1] Scott E. R. D., Taylor G. J., et al. (1993). *GRL* **20**(6): 415-418.
- [2] Warren P. H. and Kallemeyn G. W. (1992). *Icarus* **100**(1): 110-126.
- [3] Berkley J. L., Brown I., H. Gasaway, et al. (1976). *GCA* **40**(12): 1429-1430.
- [4] Berkley J. L. and Jones J. H. (1982). *JGR* **87**: A353-A364.
- [5] Berkley J. L. and Keil K. (1980). *Meteoritics* **15**(4): 264-265.
- [6] Clayton R. N. and Mayeda T. K. (1988). *GCA* **52**(5): 1313-1318.
- [7] Clayton R. N. and Mayeda T. K. (1996). *GCA* **60**(11): 1999-2017.
- [8] Walker R. J., Horan M. F., et al. (2002). *GCA* **66**(23): 4187-4201.
- [9] Goodrich C. A., Hutchison I. D., et al. (2002). *MAPS* **37**(7): A54-A54.
- [10] Downes H. and Mittlefehldt D. W. (2006). *Proc. LPSC Conf.* **37th**: #1150.
- [11] Goodrich C. A., Scott E. R. D., et al. (2004). *Chemie der Erde - Geochemistry* **64**(4): 283-327.
- [12] Chen J. H., Papanastassiou D. A., et al. (1998). *GCA* **62**(19-20): 3379-3392.

COMPARATIVE PLANETARY DIFFERENTIATION: SIDEROPHILE ELEMENT CONSTRAINTS ON THE DEPTH AND EXTENT OF MELTING ON EARLY MARS. K. Righter¹, ¹Mailcode KT, NASA Johnson Space Center, 2101 NASA Pkwy., Houston, TX 77058; kevin.righter-1@nasa.gov).

Introduction: Siderophile element concentrations in planetary mantles can provide important constraints on the conditions of core formation and differentiation in terrestrial planets [1]. Martian meteorites can be used to reconstruct mantle siderophile element concentrations for Mars. Previous efforts with this goal ([2-4]) had only small numbers (~12) of meteorite samples compared to current numbers close to 40 [5]. In addition, the Mars Exploration Rovers (MER) have provided new Ni, P, FeO and MgO data for which to compare to meteorite analyses. New meteorite and surface (MER) analyses and element correlations are used to estimate siderophile element concentrations for the martian mantle. Results are used to re-assess the conditions of metal-silicate equilibrium in Mars, especially in light of geophysical modeling [6,7]. Conditions for Mars will be compared to those proposed for Earth, Moon and Vesta.

Elements considered:

Compatible: Ni, Co, and to a lesser extent V are all compatible in olivine and chromite and thus are affected by magmatic fractionation. As a result, concentrations of Ni and Co in the mantle are strongly correlated with MgO and FeO [8,9]. Concentrations of V are correlated with Ti or Al, the former being preferred for Mars due to uncertainties with Al regarding garnet fractionation [9]. New data from shergottites as well as MER rovers define a Ni depletion (relative to chondrites) of approximately 150-200 depending upon the mantle composition (Fig. 1). Similar trends for Co and MgO+FeO define a Co depletion of 50. V depletions are defined by more primitive mantle melts due to the fractionated nature of some of the more evolved shergottites [9], and have a value of ~1 (Fig. 2).

Incompatible: These elements are incompatible during melting of a metal-free mantle, and when coupled with a refractory lithophile element of equal incompatibility, can be used to estimate mantle concentrations. Previous studies have shown similar incompatibility for the following siderophile – refractory lithophile element pairs: Mo-Pr, W-La, P-Ti, and Ga-Al. New data for shergottites define depletions for Mo of ~20, for P of ~3 (Fig. 3), and for Ga and W of ~5 (Fig. 4).

Comparison to previous estimates: The estimates here are slightly different from previous estimates based on a smaller database. For example, previous depletion for V was 0.25 [2] and now it is ~0.8 [9]; this is partly due to a better understanding of V in

mantle and magmatic processes now. And the W depletion is better defined now than it was previously with only a few shergottite data points [4].

Results of metal-silicate modelling: Metal-silicate partition coefficients for all of these elements have been parameterized using existing experimental data (see summary of [10,11,12]), and equations of the form:

$$\ln D = a \ln fO_2 + b/T + cP/T + d(nbo/t) + e \ln(1-X_s) + f.$$

Although there are some questions still about the magnitude of temperature effects (e.g., for Ni; [13]) or the valence of W ([14]), these expressions provide useful constraints on the conditions prevailing during core formation. For Mars, a few of the variables can be fixed, such as core size (21 %), silicate melt composition (nbo/t = 2.7 for peridotite), core sulfur content (X_s = 0.07), and oxygen fugacity ($\Delta IW = -1$). All of these variables can be fixed with some certainty [4], leaving pressure and temperature as the remaining variables. Varying pressure and temperature results in fits to the estimated depletions for Ni, Co, V, Mo, W, P and Ga, at PT conditions of 8.0 GPa and 1625 °C (Fig. 5). This relatively low PT result is similar to previous assessments [2,3,4], indicating a much shallower and cooler magma ocean on early Mars. This is consistent with data that suggest the preservation of geochemical anomalies in the martian mantle [15], but at odds with some modelling assumptions of a completely molten early martian mantle [6, 16].

The depletion of Ni in Earth and Mars are different by a factor of 10. High Ni contents in the terrestrial mantle have been ascribed to an early hot magma ocean. If thermal modelling and assessments point towards a hot early Mars, we must explain why Earth and Mars have totally different siderophile element signatures (esp. Ni).

References: [1] Wanke, H. (1981) *Phil. Trans. Roy. Soc. Lon. Ser. A*, 303, 287-302. [2] Treiman, A.H. et al. (1987) *Proc. 17th LPSC*, pt. 2, JGR 92, E627-E632. [3] Dreibus, G. and Wanke, H. (1985) *Meteoritics* 20, 367-381. [4] Righter, K. et al. (1998) *GCA* 62, 2167-2177. [5] *Mars Meteorite Compendium*, <http://curator.jsc.nasa.gov/antmet/mmc/index.cfm>; compiled by C. Meyer. [6] Elkins-Tanton, L.T. et al. (2005) *EPSL* 236, 1-12. [7] Reese, C.C. and Solomatinov, V.S. (2006) *Icarus* 184, 102-120. [8] Wanke, H. and Dreibus, G. (1986) in *Origin of the Moon* (Hart-

mann, Phillips, and Taylor, eds.), LPI, Houston, 649-672. [9] Righter, K. et al. (2006) Amer. Mineral., in press. [10] Righter, K. et al. (2000) GCA 64, 3581-3597. [11] Righter, K. and Drake, M.J. (1999) EPSL 171, 383-399. [12] Righter, K. and Shearer, C.K. (2003) GCA 67, 2497-2507. [13] Chabot, N.L. et al. (2004) GCA 69, 2141-2151. [14] Danielson, L.R. et al. (2006), Fall AGU abstract, in press. [15] Jones, J.H. et al. (2003) MAPS 38, 1807-1814. [16] Draper, D. and Borg, L.E. (2003) MAPS 38, 1713-1731. [17] Basaltic Volcanism Study Project (1981) Pergamon Press. [18] Newsom, H.E. (1995) AGU Geophysical Handbook Series. [19] Rieder, R., et al. (2004) Science 306, 1746-1748. [20] Gellert, R., et al. (2004) Science 305, 829-832. [21] Newsom et al. (1996) GCA 60, 1155-1168. [22] Jagoutz, E. et al. (1979) PLPSC 10th, 2031-2050.

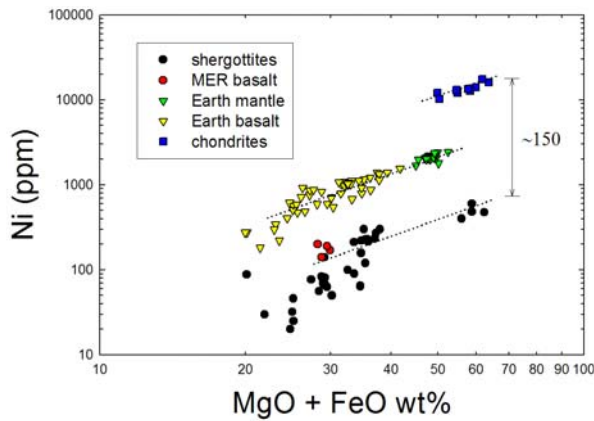


Figure 1: Ni-(MgO+FeO) trends defining depletions for the martian mantle. Data are from [17, 18, 19, 20] and references compiled by [5].

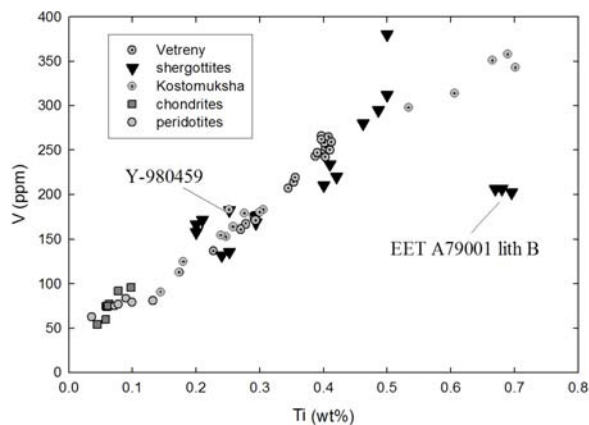


Figure 2: V - Ti trends defining no V depletion in the martian mantle compared to chondrites. Figure from [9].

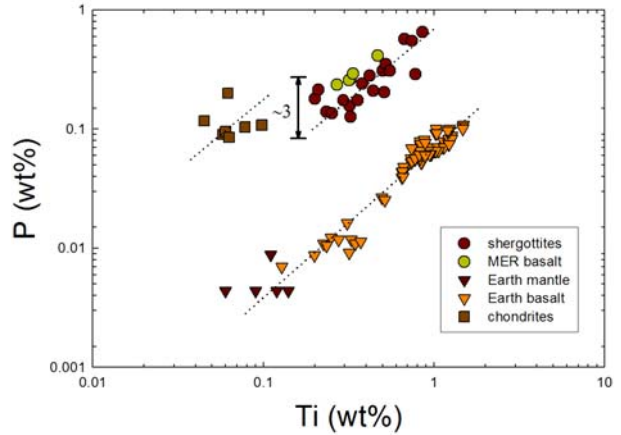


Figure 3: P-Ti trends defining a slight P depletion for the martian mantle compared to Earth. Data are from [17, 18, 19, 20] and references compiled by [5].

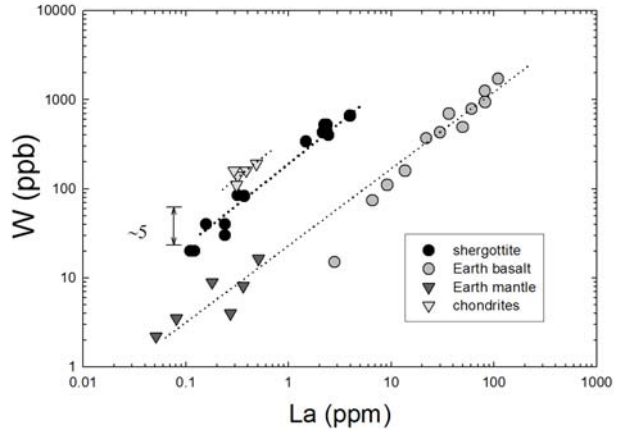


Figure 4: W-La trends defining a small depletion of W relative to chondrites. Note the small depletion compared to that defined by terrestrial samples. Data are from [18, 21, 22] and references compiled by [5].

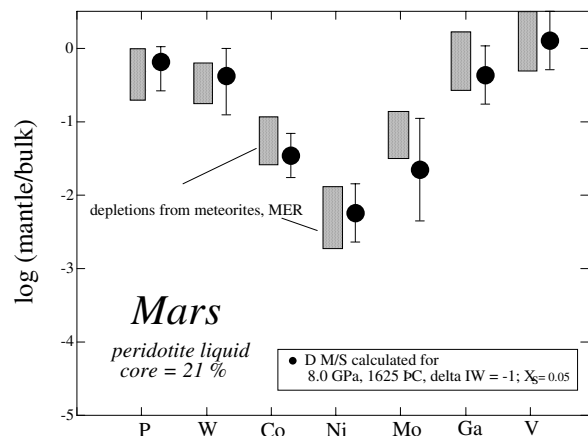


Figure 5: Comparison of calculated (shaded boxes) vs. observed depletions for Mars showing the best fit to all elements at conditions of 8 GPa and 1625 °C.

HIGHLY SIDEROPHILE ELEMENTS IN THE TERRESTRIAL UPPER MANTLE REQUIRE A LATE VENEER? NEW RESULTS FOR PALLADIUM.

K. Righter¹, M. Humayun², and L. Danielson¹ ¹Mailcode KT, NASA Johnson Space Center, 2101 NASA Parkway, Houston, TX 77058; kevin.righter-1@nasa.gov; ²National High Magnetic Field Laboratory and Dept. of Geological Sciences, Florida State University, Tallahassee, FL 32310.

Introduction: One of the most elusive geochemical aspects of the early Earth has been explaining the near chondritic relative abundances of the highly siderophile elements (HSE; Au, Re and the platinum group elements) in Earth's primitive upper mantle (PUM). Perhaps they were delivered to the Earth after core formation, by late addition of carbonaceous chondrite material [1]. However, the recognition that many moderately siderophile elements can be explained by high temperature and pressure metal-silicate equilibrium [2], leads to the question, can high temperature and pressure equilibrium similarly affect the HSE? Meanwhile, isotopic work has placed tight constraints on the Re/Os and Pt/Os of the PUM [3,4,5].

Background: In a high PT study of D(Pd) M/S (metal/silicate partition coefficient) and D(Pt) M/S, [6] showed that both partition coefficients decrease at higher pressures and temperatures, but not enough to explain the mantle concentrations of Pt or Pd by metal/silicate equilibrium. Focusing only on Pt, [7] measured the solubility of Pt in a Fe-free basalt – the diopside-anorthite system eutectic composition – to high pressures and temperatures, and found that D(Pt) M/S does not decrease enough to explain the Pt concentrations of the upper mantle. Drawbacks to these two studies included use of K- and Na-rich silicate compositions, and FeO- and S-free systems. Both of these studies were followed by experiments in systems more closely approaching that of the early Earth. D(Au) M/S decreases substantially with increased pressure and temperature, in experiments using peridotite melt and S-bearing metallic liquids [8]. D(Pt) M/S also decreases substantially at the high PT conditions and metal and silicate compositions relevant to an early magma ocean [9]. Both of these latter studies conclude that the Pt and Au concentrations in the PUM can be reconciled with a hot and liquid early terrestrial mantle equilibrating with a metallic liquid. However, conclusions for Pt rest on an interpretation that the tiny metallic nuggets plaguing many such experiments, were formed upon quench. There is not agreement on this issue, and the general question of HSE solubility at high pressures and temperature remains unresolved.

Key to resolution of this problem is the ability to work in nugget-free, uncompromised conditions, and to utilize experimental compositions that approximate those of the early Earth (i.e., peridotite and light

element bearing FeNi metallic liquid). In order to address this problem, we have undertaken a new series of experiments with the HSE Pd. Pd was chosen for two reasons. First, it is well understood at low pressures with several studies across a range of temperatures and oxygen fugacities [10,11], silicate melt compositional effects are thought to be small [11], and its behavior in S-bearing systems is well known [12]. Second, the formation of nuggets is not reported down to low fO_2 equivalent to IW-1 [10], making analysis and interpretation more straightforward than other nugget-affected elements. New experiments were conducted at high pressures at the Johnson Space Center, and analyzed for Pd at low concentration levels using LA-ICP-MS at Florida State University (FSU).

Experimental: Experiments were conducted at high pressures using both a non end-loaded piston cylinder apparatus and a multi-anvil module in an 880 ton press. The former has been calibrated using fayalite-ferrosilite equilibria and the melting point of diopside [13]. The latter has been calibrated using SiO_2 and Fe_2SiO_4 transitions in a 14/8 assembly with castable octahedra with fins, Re foil furnaces, and type C Re/W thermocouples. All experiments used MgO capsules containing natural basalt, and Fe-Pd-S-Sb alloy. The basalt reacts with the MgO to produce more magnesian homogeneous liquids, similar in composition to a komatiite or picrite. Silicate samples do not typically quench to glass (although some do), but contain a fine grained matte of silicate quench crystals. Similarly, the metallic liquid quenches to two phases – intergrown Fe-Pd-S-Sb alloy and sulfide. Run products were mounted in epoxy, cut in half along the length of the capsule, and polished for analysis.

Analytical: Run products were analyzed using a Cameca SX100 electron microprobe at NASA-JSC [13] and a New Wave UP213 (213 nm) laser ablation system coupled to a Finnigan ElementTM magnetic-sector ICP-MS at the NHMFL at FSU. The peaks ²⁵Mg, ⁵⁷Fe, ⁵⁹Co, ⁶⁰Ni, ¹⁰²Ru, ¹⁰⁵Pd, ¹⁰⁶Pd, ¹²¹Sb, ¹²³Sb, etc., were monitored in low resolution at 50 ms/peak. Silicate glasses were analyzed with an 80 μ m diameter track scanned at 10 μ m/s, and metal blobs were analyzed with 12-15 μ m diameter tracks scanned at 5 μ m/s, using 10 Hz laser repetition rate and 50% power output. The NIST SRM 1263a steel, and iron meteorites Filomena and Hoba were used as standards.

Results: Metal/silicate partition coefficients for Pd have been measured for two runs at pressures of 15 kb and temperatures of 1500 and 1700 °C. Palladium contents of the silicates and D(Pd) M/S are 0.65 and 0.40 ppm, and 73900 and 910, respectively, for the 1500 and 1700 °C runs. Because the effects of temperature, oxygen fugacity, melt composition, and metallic liquid S content are known from previous studies, we have derived an equation allowing prediction of D(Pd) M/S:

$$\ln D(\text{Pd}) = -0.232 \cdot \ln f_{\text{O}_2} + 7376/T + 8.8 \cdot \ln(1-X_s) - 0.94(\text{nbo}/t) + 7.18 \quad (\text{equation 1})$$

This expression will serve as a baseline for comparison of our new high pressure results, and allow isolation of any pressure effect. Measured and calculated $\ln D(\text{Pd})$ M/S are compared in Fig. 1. To evaluate the results of our high pressure experiments, the measured values from this study are normalized to the value calculated for the same T-fO₂-X conditions. If there is no change with pressure, the values should be close to 1; if there is a decrease or increase with pressure, they should be <1 or >1 respectively. Because both points are close to 1, pressure has only a weak effect on D(Pd) M/S. Similarly, the 4 kb and 8 kb results of [15] and [16] also are no different than the D(Pd) M/S calculated for the same T-fO₂-X conditions. Furthermore, the results of Holzheid et al (2000) [6] suggest only a weak pressure dependence to D(Pd) M/S, albeit with some scatter in their partition coefficients at any given pressure. These results are in contrast to those found for D(Ni) M/S, which decreases quickly over a small pressure range (e.g., [2]).

A P/T term can be added to equation 1 above to allow prediction of the effect of pressure on D(Pd) M/S. If a small and negative value of -20 is consistent with the pressure effect observed by this study and [6,15,16]:

$$\ln D(\text{Pd}) = -0.232 \cdot \ln f_{\text{O}_2} + 7376/T - 20 \cdot P/T + 8.8 \cdot \ln(1-X_s) - 0.94 \cdot (\text{nbo}/t) + 7.18 \quad (\text{equation 2})$$

Use of equation 2 to calculate a D(Pd) M/S at the P-T-fO₂-X conditions of 270 kb, 2000 C, $\Delta\text{IW} = -2$, $X_S = 0.05$, and $\text{nbo}/t = 2.7$ (similar to those suggested by [14] for the early Earth), results in a value of 400 (± 100), very similar to the value required for core-mantle equilibrium ($D = 600$). In fact, calculated values for even higher pressures and temperatures, suggested by [17] and [18], result in D(Pd) M/S much lower than 600, thus predicting Pd concentrations far higher than observed in the PUM.

The ease with which a low D(Pd) M/S is achieved at generally high PT conditions may be an explanation for the suprachondritic Pd/Ir ratio of the PUM [19]. This result highlights only a weak pressure effect on D(Pd) M/S, but shows that Pd [this study], Pt

[9] and Au [8] may all be consistent with a deep, early terrestrial magma ocean.

References: [1] Chou, C.L. (1978) PLPSC 9th, 219-230. [2] Walter, M.J. et al. (2000) in (R. Canup and K. Righter, eds.) Origin of the Earth and Moon, Univ. Arizona Press, 265-290. [3] Brandon, A.D. et al. (2000) GCA 64, 4083-4095. [4] Brandon, A.D. and Walker, R.J. (2005) EPSL 232, 211-230. [5] Righter, K. (2005) AGU Monograph Series 160, 201-218. [6] Holzheid, A. et al. (2000) Nature 406, 396-399. [7] Ertel, W. et al. (2006) GCA 70, 2591-2602. [8] Danielson, L.R. et al. (2005) LPSC XXXVI, #1955. [9] Cottrell, E. and Walker, D. (2006) GCA 70, 1565-1580. [10] Borisov, A. and Palme, H. (1996) Mineral. Petrol. 56, 297-312. [11] Borisov, A. et al. (1994) GCA 58, 705-716. [12] Fleet, M.E. et al. (1996) GCA 60, 2397-2412. [13] Righter, K. et al. (2006) Amer. Mineral., in press. [14] Righter, K. and Drake, M.J. (1999) EPSL 171, 383-399. [15] Peach, C.L. et al. (1994) Chem. Geol. 117, 361-377. [16] Bezmen, N.I. et al. (1994) GCA 58, 1251-1260. [17] Chabot, N.L. et al. (2004) GCA 69, 2141-2151. [18] Li, J. and Agee, C.B. (2003) GCA 65, 1821-1834. [19] Becker, H., et al. (2006) GCA 70, 4528-4550. [20] Stone, W.E. et al. (1990) GCA 54, 2341-2346.

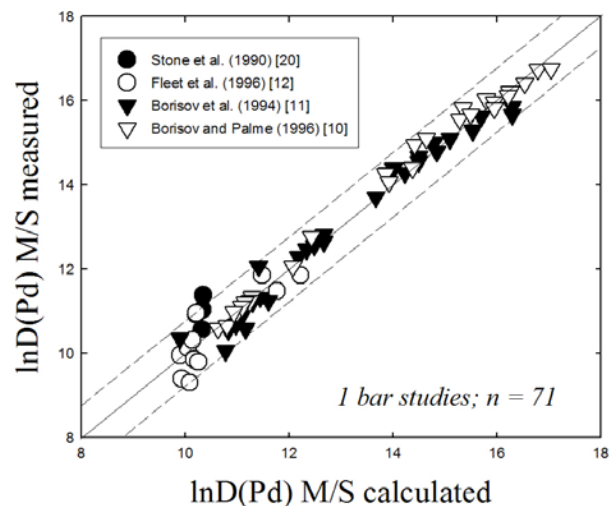


Figure 1: Comparison of $\ln D(\text{Pd})$ measured vs. calculated for the low pressure experiments of [10-12, 20]. Dashed lines are 2σ error on multiple linear regression.

PROCESSING OF THE EARTH'S UPPER CONTINENTAL CRUST BY IMPACTS OF MAGMATIC IRON METEORITES AND/OR PALLASITES: EVIDENCE FROM HSE AND NI? G. H. Schmidt^{1,2}, ¹Max-Planck-Institute of Chemistry (Otto-Hahn-Institut), Mainz, Germany (gerhard.schmidt@uni-mainz.de), ²Institute of Nuclear Chemistry, University of Mainz, Germany.

Introduction: The heavily cratered surface of the moon shows the importance of impact events in the Earth-Moon system and especially in the evolution of the Earth's crust. The HSE composition is a key issue for understanding its origin and the influence of impactors on the chemical composition of the Earth crust. However, an estimation of the average HSE composition is a difficult challenge because of the geological complexity and therefore heterogeneous composition of the exposed Earth's crust as well as the low contents in the pg/g to ng/g range. There are abundant literature data on Ir and Os analyses of continental crustal rocks, but there are only few data on Rh and Ru, primarily because of the low concentrations and difficulties with analyses. Reliable literature data on metamorphic rocks are rather rare. However, different methods involves deriving weighted averages of the present-day HSE composition of such a heterogeneous mass, e.g. from compositions of rocks exposed at the surface, from fine-grained clastic sedimentary rocks, and from glacial deposits. However, the chemistry of these elements in clastic sediments is dominated by their high density which causes segregation as metal during sedimentation.

An alternative method is to estimate upper crustal noble metal contents from impact melt samples and impactites (suevite) of large impact craters. On Earth approximately 174 impact craters up to ~300 km in diameter and up to ~2.4 Ga in age are recognized. Melts from multikilometer craters, especially from those craters where no meteoritic contamination has been detected (e.g., Mistastin, Manicouagan, Clearwater West, Nördlinger Ries) may be a good proxy for the bulk composition of a large part of the continental crust. The bulk composition of the Manicouagan impact melt have been shown to be very similar to the average chemical composition of the Canadian shield.

The impact melt sheet of the 70-85 km diameter Morokweng impact structure in southern Africa or the Clearwater East impact structure in Canada revealed high HSE concentrations [1], [2]. From such melt sheets indigenous concentrations of Os, Ru, Rh, Pt, and Pd can be derived by Ir regression lines, if the degree of PGE correlation through the melt sheet is high and assuming near-zero Ir in the indigenous component.

In this study estimates of HSE from the UCC have been inferred from impact melt samples from the Baltic Shield (Sweden) and from a large number of impactites (crater suevite) and basement rock samples from a borehole of the Nördlinger Ries impact crater. The results are compared with the HSE and Ni systematics of iron meteorites and pallasites.

The Earth's UCC is the Earth's minor repository of the compatible HSE. However, the noble metal composition of the Earth's upper continental crust is essential for understanding its origin and the fundamental processes by which it formed.

Results: The upper crustal concentration of Os and Ir may be reasonably well constrained, while considerable uncertainty remains for Ru and Rh. Estimates of noble metals of the upper continental crust have shown that elemental ratios of Os, Ir, Ru, Pt, Rh, Pd, and Ni in the upper crust are highly fractionated [3], compared to the Earth's mantle [4] and CI-chondrites (Fig.1).

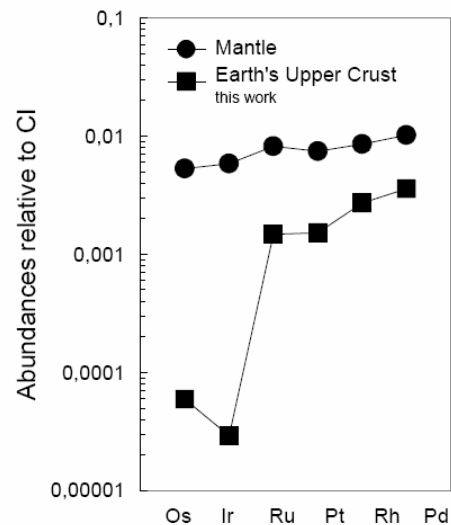


Fig. 1

The abundance distribution apparently indicates two groups of elements; (1) Os and Ir and (2) Ru, Pt, Rh, Pd, and Ni. The coherence of fractionation of the siderophile elements between two groups in the UCC suggests a cosmochemical effect

From the abundance studies of HSE in the Ries borehole and impact melt sheets from Sweden the contents of the UCC are estimated as follows: 0.03 ± 0.05 ng/g Os, 0.014 ± 0.008 ng/g Ir, 1.01 ± 0.60 ng/g Ru, 1.49 ± 0.56 ng/g Pt, 0.38 ± 0.21 ng/g Rh, and 2.00 ± 0.52 ng/g Pd (Tab. 1).

Contrasting Behaviour of HSE Abundances in the Earth's Upper Mantle and Earth's Upper Crust:

The HSE systematics of the upper mantle shows decreasing solar system normalized abundances with increasing condensation temperatures (Fig. 1), consistent with high-

temperature fractionations in the solar nebula, suggesting that these elements were added to the accreting Earth by a late bombardment after core formation.

In contrast to the mantle, the HSE pattern of the Earth's UCC is strongly fractionated (Fig. 1) with depletions in Os and Ir (by a factor up to 200) and only minor depletions in Ru, Pt, Rh, and Pd, as reflected in large variation of mantle/crust abundance ratios.

Table 3. Comparison of Os, Ir, Ru, Pt, Pd, and Ni in Earth's mantle, Earth's crust, Apollo 17 impact melt rocks, and Moon crust.

	Os ng/g	Ir ng/g	Ru ng/g	Pt ng/g	Pd ng/g	Ni µg/g	Os/Ir	Ru/Ir	Pt/Ir	Pd/Ir	Ni/Ir x10 ²
Earth's mantle											
Schmidt (2004)	2,69	2,80	5,60	7,33	5,68	1860	0,96	2,00	2,62	2,03	0,664
1σ	0,38	0,34	0,61	1,55	1,52						
Apollo 17 impact melt rocks uncorrected for indigenous contents											
Puchtel et al. (2005)	5,39	5,07	8,43	12,3	7,3		1,07	1,68	2,43	1,46	0,027 ^a
1σ	0,91	0,94	1,12	2,9	2,2		0,03	0,09	0,33	0,41	0,005
corrected for indigenous contents											
	5,39	5,07	6,42	4,4			1,06	1,27		0,88	
1σ	0,91	0,94	1,12	2,2							
Apollo 17 impact melt breccias											
Norman et al. (2002)	6,57	11,71	13,8	11,7	221			1,83	2,08	1,90	0,045
1σ	3,30	5,44	7,0	5,0	51			0,14	0,17	0,37	0,023
Earth's upper continental crust											
This work	0,03	0,014	1,01	1,49	2,00	34 ^b	2,1	72	106	143	2,429
1σ	0,05	0,008	0,60	0,56	0,52	10					
Moon crust (Apollo 17)											
Puchtel et al. (2005)	2,01		2,86	22 ^c				335		477	0,344 ^d
1σ	0,72		0,94	9							
pristine lunar rocks closest in composition to A17 melt rocks Mg-suite noritic rocks and gabbros											
Higuchi and Morgan (1975)	0,095	0,064				1,20					
CI (solar abundances)											
Palme and Jones (2003)	506	480	683	982	556	10770	1,05	1,42	2,05	1,16	0,022
1σ	25	19	20	39	56						

^aMean Ni/Ir ratios derived from Ni-Ir correlations of Apollo 17 impact melts (Palme 1980).
^bMean Ni value derived from samples of the Graded Unit (Pernicka et al. 1987).
^cMean Ni value derived from correlations of Ni and Au in Apollo 17 melt samples by Morgan et al. (2001).
^dPalme (1980) derived from correlations of Ni and Ir in Apollo 17 melt samples an indigenous value of 40±15 µg/g Ni.
^eNi/Ir ratio calculated with Ir value of 0.064 ng/g from Higuchi and Morgan (1975) and Ni value of 22 µg/g from Morgan et al. (2001).

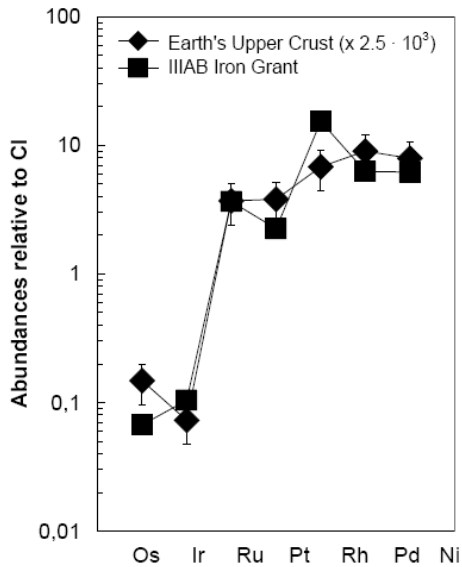


Fig. 2

The fractionated Ru/Ir ratio of about 72 in the UCC, compared to a mantle Ru/Ir ratio of 2 is difficult to explain by mantle melting, since both elements together with Os should be retained in residual mantle phases. The highly frac-

tionated Ru/Ir ratio preserved in the Earth's UCC in comparison to CI is unparalleled in terrestrial magmatic systems.

Sulfide/silicate partition coefficients for Os are very similar to those of Ru, Pd and Pt. Thus similar abundances of Os (Ir), Ru, Pd and Pt would be expected which is not observed (Fig.1). The difference between the crustal abundances of HSE suggests that during crust formation by partial melting mantle sulfides were not involved. The HSE UCC composition is difficult to explain if the crust is generated by single-stage melting of peridotitic mantle, and additional processes must therefore be involved in its generation.

The coherence of fractionation of the siderophile elements between two groups suggests a cosmochemical effect. In fact, the HSE and Ni systematics of the UCC closely resembles IIIAB iron meteorites and pallasites (Fig.2,3), probably an indication that the UCC preserves an imprint of some of the major fractionation processes which have occurred in magmatic iron meteorites or pallasites [5].

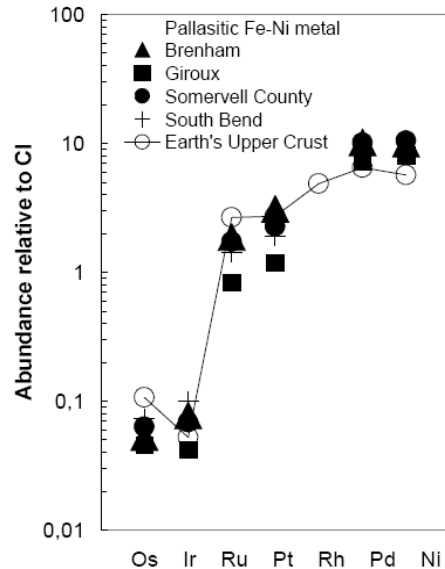


Fig. 3

References: [1] McDonald I., Andreoli M. A. G., Hart R. J. and Tredoux M. (2001) *Geochim. Cosmochim. Acta* 65:299-309. [2] Schmidt G. (1997) *M&PS* 32, 761-767. [3] Schmidt G., Palme H., and Kratz K.-L. (2005) *M&PS* 40, A135. [4] Schmidt G. (2004) *M&PS* 39, 1995-2007. [5] Schmidt G. (2006) *M&PS*, submitted.

ROLE OF PROTO-CORES IN TERRESTRIAL PLANET DIFFERENTIATION Harrison H. Schmitt¹,¹University of Wisconsin-Madison, P.O. Box 90730, Albuquerque, NM 87199 schmitt@engr.wisc.edu

Introduction: Low energy initial accretion of the terrestrial planets would create chondritic proto-cores. Magma oceans would form on these proto-cores as accretionary kinetic and potential energy were released as heat. Such a proto-core, largely undifferentiated and about 1200km in radius, appears to exist in the Moon beneath that body's upper mantle.ⁱ

Lunar Proto-core: Seismic data from Apollo seismometers indicate that the base of the near-side upper mantle of the Moon lies about 550km below the surface and is underlain by a lower mantle that is apparently more aluminum-rich.ⁱⁱ The high volatile content and chondritic isotopic ratios of the non-glass components of the Apollo 15 green and Apollo 17 orange pyroclastic glasses strongly suggest that the upper portion of the lower mantle also is largely undifferentiated, chondritic material. Evidence from Apollo lunar samples, lunar meteorites and remote sensing data from the Apollo 15-16, Clementine and Lunar Prospector missions indicates that the mafic upper mantle fractionally crystallized from an originally chondritic magma ocean.ⁱⁱⁱ A ferro-anorthositic crust that averages about 60km thick, globally, overlies the mantle.^{iv}

Consequences for Core: Core-forming material, separated as an immiscible liquid from the lunar magma ocean 25-30 Myr after T_0 ^v, could not have immediately formed a core due existence of a relatively cool, silicate dominated lunar proto-core. The proto-core would have delayed to some extent the migration of core-forming material to the center of the Moon. The existence of far-side magnetic anomalies antipodal to the youngest of the large lunar basins^{vi} suggests that a lunar core dynamo did not form until about 3.9 Ga. That date also may be the approximate time of the aggregation of sufficient liquid core-forming material to allow a temporary dynamo to exist.

Implications: This clear suggestion of a ~600 Myr delay in lunar core formation should prompt the examination of data on other terrestrial planets for similar delays probably varying inversely with size, that is the delay for Mars would be less than that for the Moon and more than that for the Earth. With respect to Mars, it appears that a core dynamo existed only prior to the initiation of very large basin formation as the formation of the 2000km diameter Hallas basin disrupted the magnetic striping in the Southern Uplands.^{vii} Thus, a Martian dynamo would have formed prior to the initiation of large basin formation,

whereas, the lunar dynamo only was present at the end of this period.

1 Ahrens, T. J. (1991) in C. B. Agee and J. Longhi, eds., *Workshop on the Physics and Chemistry of Magma Oceans from 1 Bar to 4 Mbar*, Technical Report Number 92-03, Lunar and Planetary Institute, Houston, 13-14; Schmitt, H.H., (2003) in H. Mark, editor, *Encyclopedia of Space and Space Technology*, Wiley, New York.

2 Hood, L. L. and M. T. Zuber (2000) in R. M., Canup and K. Righter, Eds., Arizona Press, Tucson, and LPI, Houston, 397-409.

3 Wood, J. A. et al (1970) *LPSI* 1, 965-988; Smith, J. V. et al (1970) *LPSI*, 897-925; Jones, J. and H. Palme (2000) in R. M., Canup and K. Righter, Eds. Arizona Press, Tucson, and LPI, Houston, 205-209.

4 Wiezorek, M. A., and R. J. Phillips (1998) *JGR* 103, 1715-1724; Hood, L. L., and M. T. Zuber (2000) in R. M., Canup and K. Righter, Eds., Arizona Press, Tucson, and LPI, Houston, , p 400.

5 Kline, T., et al (2002) *Nature*, 418, 952-955.

6 Lin, R. P., and co-workers, *Science*, 281, 1998, p 1481; Lin, R.P., and co-workers, *Lunar and Planetary Science Conference 30*, Abstract #1930, 1999; Mitchell, D. L., and co-workers, *Lunar and Planetary Science Conference 31*, Abstract #2088, 2000.

7 Connerney, J. E. P., and co-workers, *Science*, 284, pp 794-798.

POSSIBLE CORE FORMATION WITHIN PLANETESIMALS DUE TO PERMEABLE FLOW. H. Senshu¹ and T. Matsui², ¹Tokyo Institute of Technology (2-12-1 Ookayama, Meguro-ku, Tokyo, JAPAN, 152-8541, senshu@geo.titech.ac.jp), ²University of Tokyo (5-1-5 Kashiwanoha, Kashiwa-City, Chiba, JAPAN, 277-8562).

Introduction: The study on the early thermal evolution of small celestial bodies with the size from a few kilometers to about hundred kilometers is important not only because the parent bodies of meteorites are thought to be the similar size but also because the proto-planets had formed by accretion of such sized bodies (planetesimals). Planetesimals and parent bodies of meteorites are thought to have formed by gathering dust by gravitational instability in a short time scale. They were too small to evolve thermally by accretional energy, but instead, short-lived radioisotopes should have played important roles in the early thermal evolution. As a result the thermal evolution of small sized body is decided by the balance between internal heating and radiative cooling from the surface.

If the internal temperature exceeds the solidus temperature of metal, the molten metal could separate from silicate. Yoshino *et al.* [1] carried out the laboratory experiment to confirm whether percolation of molten metal on silicate grains could take place or not. They showed that if the metal contains enough sulfur and the volume fraction of metal exceeds a threshold value the molten metal can connect with each other to form 'pipe' through which molten metal can migrate along the gravity.

Thus we constructed a one-dimensional early thermal evolution model of planetesimals. The goal of this study is to clarify the condition for planetesimals to form a metallic core.

Model: Our model considers the internal heating due to the decay of short-lived radioisotopes, cooling from the surface, porosity-dependent thermal conductivity, and silicate-metal separation due to permeable flow, if the temperature exceeds the solidus temperature of metal. Since the solidus temperature of metallic alloy highly depends on the sulfur content, we also consider the change of sulfur content along the phase diagram of Fe-FeS system [2]. The bulk composition of the planetesimal is calculated by using two-component model [3, 4]. The heat sources considered in this model are ²⁶Al and ⁶⁰Fe, and their abundances at the time of CAI formation are taken from [5] and [6], respectively.

The flow speed of molten metal is calculated as follows:

$$v = K \frac{\Delta\rho}{\mu} \frac{\partial P}{\partial z}$$

where K is the permeability of silicate media, $\Delta\rho$ is the density difference between molten metal and silicate, P is the hydrostatic pressure, μ is the viscosity of molten metal, respectively. The permeability is given as a function of the porosity ϕ and the grain size of silicate media, G , as follows:

$$K = \frac{\phi^2 G^2}{200}$$

The porosity-dependence of thermal conductivity and the shrinkage of pores by sintering due to pressure and temperature are given from [7] and [8], respectively.

The key parameters in this model are the mass of planetesimal, the grain size of silicate media, and the initiation time of thermal evolution. We vary these parameters to study the dependency of numerical results.

Results: Figure 1 shows one of the numerical results, for the case that the initial time of the thermal evolution is 1Myr after the CAI formation, the mass of the planetesimal is 10^{16} kg, and the grain size of silicate media is 10^{-3} m. We can see the shrinkage of radius due to sintering about 100kyr after the initiation of thermal evolution, the core formation about 500kyr after the initiation, and the formation of partial melting zone at the center 1Myr after the initiation.

We carried out the numerical simulation of thermal evolution for various masses of planetesimals, initiation times, and grain sizes of silicate. According to our result, planetesimals form metallic core when the grain size of silicate media is larger than 10^{-4} m and the mass of the planetesimal is larger than about 2×10^{15} kg, if the initiation time of thermal evolution is 1Myr after CAI formation. These conditions are to be satisfied to achieve sufficient flow speed of permeable flow and solidus temperature of metallic alloy, respectively. Figure 2 shows the condition for core formation as a function of the size of the planetesimal and the initiation time of thermal evolution after CAI formation. There are two conditions to be satisfied to form core: initiation time is to be less than 2Myr to contain sufficient heat source and the mass of the planetesimal is to be larger than a critical value to retain the heat depending on the initiation time.

Summary: Our numerical results show that there are obvious conditions to be satisfied to form metallic

core at the center of the planetesimals. The initiation time should be within 2Myr since CAI formation and the mass of the planetesimal should be larger than 10^{16} kg, or the radius of the planetesimal should be larger than 10km, which is equivalent to the typical size of planetesimals formed by gravitational instability within solar nebula [9,10] and also equivalent to the size of parent body of iron meteorites [11].

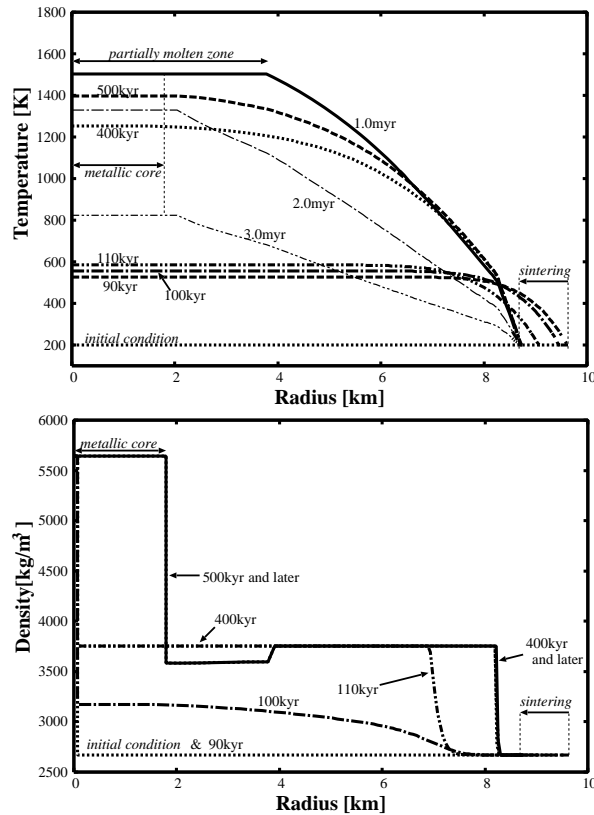


Figure 1: evolution of thermal (top) and density (bottom) structure of a planetesimal with the mass of 10^{16} kg, the initiation time of 10^6 yr after CAI formation, and the grain size of 10^{-3} m. Numerals beside each curve represent the time since the thermal evolution started.

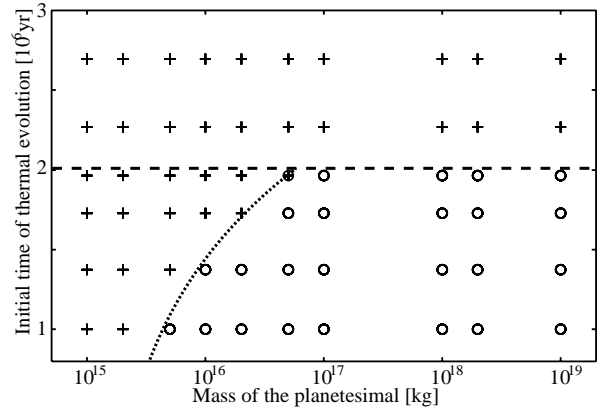


Figure 2: whether a metallic core formed or not as a function of the mass of the planetesimal and the initiation time of thermal evolution. Crosses represent the condition under which no metallic core formed while open circles represent the condition under which a metallic core formed.

References: [1] Yoshino, T. *et al.* (2003) *Nature*, 422, 154. [2] Kullerud, G. (1967) in “*Research in Geochemistry*”, 286-321. [3] Ringwood, A. E. (1977) *Geochem. J.*, 11, 111. [4] Dreibus, G. and H. Wänke (1987) in “*Origin and Evolution of Planetary and Satellite Atmospheres*”, 268-288. [5] MacPherson, G. J. *et al.* (1995) *Meteorit.*, 30, 365. [6] Tachibana, S. and G. R. Huss (2003) *Astrophys. J.*, 588, L41. [7] Yomogida, K. and T. Matsui (1983), *J. Geophys. Res.*, 88, 9513. [8] Yomogida, K. and T. Matsui, (1984), *Earth Planet. Sci. Lett.*, 68, 34. [9] Safronov, V. S. (1969) in “*Evolution of protoplanetary cloud and formation of the Earth*”, 1-206. [10] Goldreich, P. M. and W. R. Ward (1973) *Astrophys. J.*, 183, 1051. [11] Mittlefehldt, D. W. *et al.* (1998) *Rev. Mineral.*, 36, 4-1-195

Remnants of a Magma Ocean. Insights into the Early Differentiation of the Moon and its Relevance to the Differentiation of the Terrestrial Planets. C.K. Shearer, Institute of Meteoritics, Department of Earth and Planetary Sciences, University of New Mexico, Albuquerque, New Mexico 87131-0001.

Introduction: The Moon has been and will continue to be the scientific foundation for our understanding of the early evolution of the terrestrial planets. The detailed geologic record of these early events has long since vanished from the Earth and has been at least partially erased from Mars. The Moon contains the remnants of one of the basic mechanisms of early planetary differentiation: magma ocean (MO) [e.g., 1, 2, 3]. These remnants consist of a primary planetary crust and subsequent crustal additions that were products of melting of MO cumulates in the lunar mantle. The intent of this presentation is to discuss recent insights into the early differentiation of the Moon, inadequacies in our current perception of lunar differentiation, and the relevance of the Moon to understanding the differentiation of the terrestrial planets.

Examples of recent insights:

Duration of Lunar Magma Ocean (LMO) Crystallization. Although initially hampered by cosmogenic production of W^{182} , Hf-W chronometry has been interpreted as indicating that the LMO crystallized over a period of 20 to 50 million years [e.g. 4, 5, 6, 7]. This contrasts with proposed thermal models for the crystallization of the LMO [8] and some Sm-Nd and Rb-Sr model ages for the last dregs of lunar magma ocean crystallization: urKREEP [9, 10, 11]. However, by combining ^{147}Sm - ^{143}Nd data for a young KREEP-enriched basalt (NWA733) with data from older "KREEP magmatic lithologies" (Mg-suite, KREEP basalts, high-Al basalts), Borg et al. [12], Borg and Wadhwa [13], and Edmunson et al. [14] recalculated the model age for urKREEP. This new model age suggests that the crystallization of urKREEP occurred at 4.492 ± 0.061 Ga. The ^{147}Sm - ^{143}Nd [12, 13, 14] and Hf-W data sets are consistent with each other and imply a rapid crystallization of the LMO. A further interpretation of this data is that a significant portion of the LMO crystallized very rapidly (5-10 my), whereas the very last dregs (KREEP > 99% crystallization of the LMO), containing high abundances of heat-producing elements and insulated by a thick primary crust of ferroan anorthosite (FAN), crystallized much slower.

Conceptually, most models for the crystallization of the LMO advocate the generation of a primary FAN crust that was subsequently invaded by episodes of basaltic magmatism produced by melting of distinct LMO cumulate packages. The thick primary crust isolated the lunar mantle from the addition of siderophile elements via "late-veener" [15]. The time of transition from LMO crust formation to post-LMO crustal

growth should be distinct yet there is substantial overlap in ages between primary and secondary crustal lithologies [16]. Some of this interpretive problem is tied to the early impact environment of the Moon and the mineralogical-chemical character of the FAN lithologies. A relative geochemical timescale of LMO processes can be established by Ti/Sm and Ti/Y [17, 18, 19, 20]. These geochemical ratios indicate a petrogenetic sequence of very-low and low-Ti LMO cumulates \Rightarrow FAN \Rightarrow high-Ti LMO cumulates \Rightarrow urKREEP \Rightarrow Mg-suite. The Mg-suite represents the first stage of post-LMO crustal building.

LMO Cumulate Lithologies and Interactions. Lunar magmas are produced from melting of a wide compositional range of different LMO cumulate packages. The Mg-suite represents melting of cumulate sources distinctly different from mare basalt sources. Compared to mare sources, Mg-suite sources had a higher Mg' and lower abundances of Ni, Co, and Cr [20]. The high Mg' suggests that the magmas that produced the Mg-suite were derived from melting of the deep LMO cumulate pile (with the addition of KREEP by assimilation or mixing). This appears to contradict the low Ni and Co [2, 3, 16, 20, 21]. However, parameterization of Ni behavior by Jones [22] and experimental studies by Longhi and Walker [23] demonstrated that D^{ol-liq}_{NiO} is low at low values of D^{ol-liq}_{MgO} . Therefore, complete melting of a bulk planetary composition (\approx peridotite) will yield the lowest value of D^{ol-liq}_{MgO} and consequently, the lowest values of D^{ol-liq}_{NiO} (≈ 1) during the crystallization of the first MO cumulates [23]. If correct, the LMO cumulates from which the Mg-suite magmas were derived best approximate the concentrations of Co and Ni in the LMO.

Examples of Inadequacies of LMO models:

There are numerous inadequacies in our fundamental understanding of the differentiation of the Moon.

Petrogenesis of FANs. Our concepts for the formation of continental size masses of plagioclase flotation cumulates is still in its infancy. Combining (1) comprehensive models for the behavior of plagioclase during the latter stages of LMO crystallization, (2) distribution and character of the primary FAN crust, and (3) isotopic and trace element characteristics of FANs would be a reasonable first step.

Sampling of the Moon. The Moon is very asymmetric with regards to the distribution of mare basalts, heat-producing elements (KREEP, Th), and primary FAN crust. There are also terrains that are not repre-

sented in current lunar sample collections (i.e., Aitken basin). As the Apollo and Luna missions returned samples from a fairly limited geologic terrain in and adjacent to the Procellarum KREEP terrain, many of our models for lunar differentiation are based on a limited sampling of the Moon. Ryder et al. [24] and Shearer and Borg [25] identified lunar sites that could be sampled in the future to provide a more comprehensive view of the differentiation of the Moon.

Lunar Interior. Although the Apollo seismic network provided us with a glimpse of the lunar interior, the clustering of seismometers on the nearside of the Moon resulted in significant ambiguities in the interpretation of the seismic data. The 560 km seismic discontinuity has been interpreted as the base of the LMO or the transition between early olivine-rich LMO cumulate and subsequent orthopyroxene-rich LMO cumulates [26,27]. Recent inversions of several geophysical data sets cannot differentiate between a partially molten Fe-FeS-C core with a radius less than 375 km and a slightly larger partially molten silicate core [27]. A much more extensive geophysical network would allow us to better view the lunar interior and the anatomy of the LMO.

Relevance of the Moon to the differentiation of the terrestrial planets.

Clearly, the differences in size and style of accretion between the Moon and other terrestrial planets have affected the pathways of early planetary differentiation. Nevertheless, the Moon provides a valuable and nearly complete end-member record for a style of planetary differentiation. The similarities and contrasts with the other terrestrial planets provide a meaningful road to travel to understand planetary differentiation as it applies to all planetary settings.

The Moon illustrates that planetary differentiation occurs fairly rapidly over 10s of millions of years. Apparent differences between the Moon and Mars in $\epsilon^{142}\text{Nd}$ require differences in the timing of differentiation or the efficiency of MO crystallization [10,13,14,28,29]. This needs to be explored further. The mantle reservoirs produced during initial stages of differentiation may be preserved for the lifetime of that planetary body and contribute to subsequent periods of magmatism.

Contrasts in density of the MO cumulate pile may contribute to the initial dynamics of early planetary mantles and the first stages of post-MO magmatism.

Pressure regimes under which MO crystallize have a profound effect on composition and mineralogy of primary planetary crusts, cumulate lithologies, and final residual liquids. The primary crust of 4 Vesta is dominated by basalts, the Moon by FANs [1,2,3,16,20,21,30] and Mars possibly by pyroxene-

dominated assemblages (i.e., ALH84001) [28]. The early crystallization of garnet from the martian MO [28] strongly influenced the absence of plagioclase on the MO liquidus and the $\text{CaO}/\text{Al}_2\text{O}_3$ of the MO (+cumulates). The nature of the primary crust produced during MO evolution dictates the extent the “late-veener” contributed to planetary mantles. The development of a thick and rigid FAN crust isolated the lunar mantle from contributions from late-stage accretion, whereas on Earth the “late-veener” was incorporated into the mantle [15].

Late-stage liquid products of MO crystallization are strikingly similar between those estimated for the Moon (urKREEP) [3] and calculated for Mars (end-member source component for the enriched shergottites) [3,27,28]. Differences reflect the appearance of plagioclase as a LMO liquidus phase and MO bulk compositions (K, Na, Rb, Cs, H_2O). Further, the urKREEP signature is significantly more visible on the lunar surface.

References

- [1] Wood et al. (1970) Proc. 1st LSC 965-988. [2] Longhi (1980) Proc. 11th LPSC 289-315. [3] Warren (1985) Ann. Rev. Earth Planet. Sci. 13, 201-240. [4] Lee et al., (1997) Science 278, 1098-1101. [5] Shearer and Newsom (2000) GCA 64, 3599-3609. [6] Righter and Shearer (2003) GCA 67, 2497-2503. [7] Kleine et al. (2005) Science 310, 1671-1674. [8] Solomon and Longhi (1977) Proc. 8th LPSC 583-599. [9] Carlson and Lugmair (1979) EPSL 45, 123-132. [10] Nyquist et al. (1995) GCA 59, 2817-2837. [11] Nyquist and Shih (1992) GCA 56, 2213-2234. [12] Borg et al. (2004) Nature 432, 209-211. [13] Borg and Wadhwa (2006) LPSC XXXVII, abst.# 1154 [14] Edmunson et al. (2006) EPD 2006, this volume. [15] Walker et al. (2004) EPSL 224, 399-413. [16] Shearer et al. (2006) *In: New Views of the Moon* (eds. Jolliff, Wieczorek, Shearer, and Neal) 365-518. [17] McCallum and Charette (1978) GCA 42, 859-870. [18] Norman and Ryder (1980) Proc. 11th LPSC, 317-331. [19] McKay et al. (1978) Proc. 9th LPSC, 661-687. [20] Shearer and Papike (2005)GCA 69, 3445-3461. [21] Taylor and Jakes (1974) Proc. 5th LSC, 1287-1305. [22] Jones (1995) AGU Reference Shelf 3, 73-105. [23] Longhi and Walker (2006) LPSC XXXVII, abst. # 2452. [24] Ryder et al. (1989) EOS 70, 1495-1509. [25] Shearer and Borg (2006) Chemie der Erde Geochem. 66, 163-185. [26] Hood and Zuber (2000) *In: Origin of the Earth and Moon* (eds. Canup and Righter). [27] Khan et al. (2006) Geophys. J. Int. (in press). [28] Borg and Draper (2003) MAPS 38, 1713-1731. [29] Rankenburg et al. (2006) 69th Annual MetSoc. Abst.# 5036. [30] Snyder et al. (1992) GCA 56, 3809-3823.

Exploring the Differentiation of the Terrestrial Planets through Future Sample Return Missions to the Moon and Construction of a Lunar Geophysical Network. C.K. Shearer¹, C. Neal², L. Borg³, and B. Jolliff⁴. ¹Institute of Meteoritics, Department of Earth and Planetary Sciences, University of New Mexico, Albuquerque, New Mexico 87131-0001 (cshearer@unm.edu). ²Department of Civil Eng. & Geological Sciences, University of Notre Dame, Notre Dame, Indiana 46566, ³Lawrence Livermore National Laboratory, Livermore, CA 94551. ⁴Department of Earth and Planetary Sciences, Washington University, St. Louis, Missouri 63130-4899.

Introduction: Human and robotic exploration of the Moon has been fundamental to our understanding of the differentiation of the terrestrial planets [e.g., 1-9]. Yet, there still remains a variety of questions with regards to this fundamental planetary process: (1) What is the lateral and vertical extent of this initial differentiation (whole Moon or partial Moon melting)? (2) To what extent is the anatomy of early lunar differentiation preserved in the current internal structure of the Moon? (3) What is the true nature of the primary lunar crust at depth and outside of the Procellarum KREEP Terrane (PKT)? (4) Is early differentiation through magma ocean formation and crystallization unique to the Moon or is it a common process to all of the terrestrial planets? (5) Is the asymmetry observed in the lunar crust a reflection of mantle asymmetry? (6) How do the unsampled and unique lunar terranes, such as the Aitken basin, fit into our concept of lunar differentiation? Here, we illustrate two approaches for gaining a more rigorous understanding of the early differentiation of the Moon and the other terrestrial planets: additional sampling of the Moon and building a lunar geophysical network.

Sample Return and the Differentiation of the Moon.

Introduction. The Moon is very asymmetric with regards to the distribution of mare basalts, heat-producing elements (KREEP, Th), and primary ferroan anorthositic (FAN) crust. Further, there are terranes that are not represented in the Apollo, Luna, or lunar meteorite sample collections (i.e., Aitken basin). As the Apollo and Luna missions returned samples from a fairly limited geologic region in and adjacent to the PKT, many of our models for lunar differentiation are based on a limited, even biased sampling of the Moon.

Importance of Samples. Samples returned from the surface of the Moon are both complementary to orbital and in situ observations and provide a unique perspective for understanding the nature and evolution of that body. This unique perspective is based on the scale the sample is viewed (mm to angstroms), the ability to manipulate the sample, the capability to analyze the sample at high precision and accuracy, and the ability to significantly modify experiments/analyses as logic and technology dictates over an extended period of time (decades). The importance of samples is that they yield information fundamental to the understanding of

a planetary body that cannot be obtained in any other way. The discussions in this workshop illustrate the importance of samples in understanding the early evolution of the Earth-Moon system.

Sample return has a symbiotic relationship with orbital science and surface science. Returned samples are scientifically more valuable if they can be placed within a planetary context through orbital observations and if information concerning planetary-scale processes and conditions can be extracted from them. Conversely, samples give remotely-sensed data ground truth, in that they act as a "calibration standard" for these data allowing a much enhanced global view to be constructed.

Sample Size. The size of samples returned from the Moon in the future will be highly dependent upon the lunar surface exploration strategy. This strategy could include robotic, human, or integrated human-robotic sample return. Robotic sample return may be useful in exploring unique lunar terranes either prior to or in conjunction with initial human sorties. Although this approach would return small sample volumes, numerous terranes could be sampled in a cost-effective means (relative to human missions) and the resulting information could be utilized to identify sites for human sorties. Lessons learned from the Apollo missions and associated science documents the important science that can be extracted from small samples relevant to early differentiation [10]. In most cases to address many of the questions posed in the introduction, a carefully selected sample mass of 1 kg would be adequate to perform a wide-range of mineralogical, geochemical, and isotopic analyses, as well as preserving samples for future analysis to take advantage of technological advances in analytical instrumentation. This volume of material could consist of 100 to 500 individual samples that are greater than 1 gram. One exception could be primary, plagioclase-rich crust (FAN) from the far-side. The low elemental abundances of incompatible elements such as the REE and nearly monomineralic characteristics of these early lithologies may demand larger sample masses for critical isotopic analysis.

Potential sampling sites relevant to understanding lunar differentiation. Ryder et al. [11] and Shearer and Borg [10] identified lunar sites that could be sampled in the future to provide a more comprehensive view of the differentiation of the Moon. Critical samples to

return and analyze would be representative lithologies from (1) the far-side “primary crust” exposed in central peaks (Tsiolkovsky), (2) deep crustal lithologies outside the regions sampled by Apollo that occur in large impact craters/basins (Aitken basin), (3) mare basalts that represent the youngest episodes of mare volcanism (Roris basalt in Oceanus Procellarum), (4) large, fire-fountaining deposits that may contain mantle xenoliths (Rima Bode, Aristarchus plateau), (5) old mare basalt deposits (Schickard), (6) typical far-side mare basalts (Mare Moscoviense), and (7) far-side Mg-suite plutons exposed on crater floors (Hertzprung). These samples will allow us to better understand the Moon-wide nature of the primordial lunar crust and the character of the lunar mantle beneath other lunar terranes.

Geophysical Networks.

Introduction. As demonstrated on Earth, geophysical networks give invaluable information concerning the mineralogy, geochemistry, structure, and dynamics of a planet’s interior. Although the Apollo passive seismic network provided us with a glimpse of the lunar interior, the clustering of seismometers on the near-side of the Moon resulted in significant ambiguities in the interpretation of the deep lunar interior [12-14]. The 560 km seismic discontinuity has been interpreted as the base of the LMO or the transition between early olivine-rich LMO cumulate and subsequent orthopyroxene-rich LMO cumulates [12,13]. However, the resolution of the seismic data is such that the mantle beneath this has been postulated to either contain a greater proportion of Mg-rich olivine or a small proportion of garnet. While such interpretations cannot be resolved using the current seismic dataset, the different mineralogies postulated have profound implications for the bulk composition of the Moon. Recent inversions of several geophysical data sets cannot differentiate between a partially molten Fe-FeS-C core with a radius less than 375 km and a slightly larger partially molten silicate core [13].

Seismic Network. A network of approximately 10 widely dispersed, short-period seismometers operating for a 5-10 year period of time would provide data upon which to make much improved estimates of the crustal thickness of diverse terranes, provide estimates of the thickness and distribution of primary lunar crust, constrain the composition, size, and physical state of the lunar core, further constrain the seismic structure of the lunar mantle, and determine if the mantle structure varies beneath the major geologic terranes [14-16]. All of these observations are critical for reconstructing the interior of the Moon as it pertains to early differentiation. A single, long-period seismometer operating on the lunar surface for 1-2 years to measure lunar free

oscillations (shallow moonquakes, meteoroid impacts) would increase our knowledge of both the density and rigidity structure of the Moon [16].

Heat flow measurements. Heat flow measurements were made at the Apollo 15 and 17 sites that straddle the PKT and feldspathic highlands terrane [16]. It is uncertain if these measurements accurately represent either terrane or the heat flow of the Moon as a whole. Measuring heat flow at disperse locations (associated with seismic stations) would improve our understanding of the distribution of radioactive elements and help delineate terrane boundaries [16]. Both would lead to a clearer view of the structure and evolution of the magma ocean.

Magnetism: Surface magnetometer measurements made during Apollo were obtained at locations that were not ideal for testing hypotheses about the origin of the lunar crustal magnetic field. Any future magnetometer deployments should be at the sites of known strong magnetic anomalies. The first deployments should be on the near side where the surface geology is relatively well understood. For example, deployments at the Descartes mountains and the Reiner Gamma sites would directly address the following questions: (a) What are the sources of lunar magnetic anomalies? and (b) What is the origin of the Reiner Gamma-type albedo markings? The first question has implications for the origin of the magnetizing field(s) since deep-seated sources would strongly suggest a core dynamo while surficial, rapidly forming sources would allow the possibility of transient fields (as well as a core dynamo). The second question has implications for the causes of optical maturation on airless silicate bodies in the inner solar system.

References

- [1] Wood et al. (1970) Proc. 1st LSC 965-988. [2] Longhi (1980) Proc. 11th LPSC 289-315. [3] Warren (1985) Ann. Rev. Earth Planet. Sci. 13, 201-240. [4] Lee et al., (1997) Science 278, 1098-1101. [5] Carlson and Lugmair (1979) EPSL 45, 123-132. [6] Righter and Shearer (2003) GCA 67, 2497-2503. [7] Kleine et al. (2005) Science 310, 1671-1674. [8] Solomon and Longhi (1977) Proc. 8th LPSC 583-599. [9] Nyquist and Shih (1992) GCA 56, 2213-2234. [10] Shearer and Borg (2006) Chemie der Erde Geochem. 66, 163-185. [11] Ryder et al. (1989) EOS 70, 1495-1509. [12] Hood and Zuber (2000) *In*; Origin of the Earth and Moon (eds. Canup and Righter). [13] Khan et al. (2006) Geophys. J. Int. (in press). [14] Neal (2006) Geotimes 51, 30-35. [15] Neal et al. (2004) LPSC XXXV, abst.# 2093. [16] Wiczorek et al. (2006) *In*: New Views of the Moon (eds. Jolliff, Wiczorek, Shearer, and Neal) 365-518.

EARLY PLANETARY DIFFERENTIATION: AN OVERVIEW. D. J. Stevenson, Caltech 150-21, Pasadena, CA 91125; djs@gps.caltech.edu

Introduction: This overview talk necessarily touches on all the themes of the meeting. Terrestrial planets are differentiated into core and mantle because they contain immiscible ingredients (metallic iron-rich alloy and silicates) and because sufficient heat was supplied to cause extensive melting and allow gravity to separate these ingredients. Additional differentiation (inner core, crust, possible mantle layering) is small by comparison. Other explanations for the primary differentiation (extremely heterogeneous accretion, differentiation of solids from solids by viscous flow) are implausible.

Primordial Dominates: The primary differentiation is also primordial in nearly all cases because of the large energy supplied by accretion, larger than all subsequent radiogenic heat release for all bodies bigger than about the Moon. Differentiation (of iron from silicates) can be delayed by a billion years or more in bodies such as Ganymede or Titan because accretional heating is buffered by ice and radiogenic heat is needed. Heating during accretion is not only large for large terrestrial planets, it may also be delivered in a small number of highly traumatic events (giant impacts) thus reducing the ability of the planet to eliminate the heat by subsolidus convection or a hot atmosphere. The Moon is a special case because some of its initial heat may be inherited from a giant impact on Earth that was a necessary precursor to lunar formation. Mars might also be a special case if it managed to avoid a giant impact and is instead an embryo from an early stage of runaway accretion. Mercury may have been unusually hot if the explanation for the iron-poor composition is a nearly head on giant impact that blasted off much of the silicate mantle.

Magma Oceans: Despite possible special cases it seems likely that all terrestrial planets had magma oceans because of the inability to eliminate the large heat input in the short timescale characterizing planetary accumulation (less than a hundred million years). Although it is popular to think of this magma ocean environment as well defined (typical depth, etc) this is unlikely to be true; instead, the evolution of such an ocean is highly dynamic depending on the sequence of events that injected its heat budget. Still, this forms the environment in which part of the core formation takes place and part of the primordial establishment of geochemical reservoirs (e.g., partial mantle differentiation) may take place.

Liquid Cores: We now have good reason to suspect that all the terrestrial planets have at least partially liquid cores, though the evidence for Venus remains weak. The separation of core from mantle is fluid dynamically rather easy to accomplish, although many aspects of this remain imperfectly understood.

Mantle Differentiation: Differentiation within the silicate component presents some considerable issues and uncertainties because the thermal energy budget and associated buoyancy is probably sufficient in principle to keep things well stirred. The most likely scenario for differentiation in this circumstance is the one that currently allows basaltic magma to escape: Percolative flow of a primarily solid medium. But even so, the resulting crust (or D'' or whatever) can be recycled and its preservation is sensitively dependent on the subsequent planetary history.

The Legacy: The evident legacy of early differentiation for Earth is the core superheat (the fact that the specific entropy of the core is well in excess of the value appropriate to a core-forming alloy in equilibrium with the mantle), the siderophile abundances, possibly D'' for Earth, possibly mantle layering in Mars, possibly the lack of basalts on Mercury. Geochemistry and cosmochemistry guided by realistic physical modeling is central to understanding this.

Unresolved Questions: Among the unresolved questions that one would hope to see discussed at this meeting or in discussion of this overview are these: What is the role of chance (e.g., in setting up different evolutionary paths for Venus and Earth), what is the origin and role of volatiles (especially water), is there significant undifferentiation (e.g., assimilation of materials from the core back into the mantle), what is the role of small bodies (rather than giant impacts) in the accretional process, what is the role of pressure and resulting shifts in phase equilibria for the silicate assemblage, and to what extent Earth has a poor memory of ancient events because plate tectonics is good at obliterating the record?

¹⁷⁶Lu-¹⁷⁶Hf IN LUNAR ZIRCONS: IDENTIFICATION OF AN EARLY ENRICHED RESERVOIR ON THE MOON D.J. Taylor¹, K.D. McKeegan¹, T.M. Harrison^{1,2}, and M. McCulloch², ¹Dept. of Earth and Space Sciences & IGPP, UCLA, Los Angeles, CA, 90095, dtaylor@ess.ucla.edu. ²Research School of Earth Sciences, Australian National University, Canberra, A.C.T. 0200 AUSTRALIA

Introduction: The mantle and crust of the Moon have preserved the earliest phase of planetary differentiation, yet a precise chronology and understanding of the development of primordial lunar crust has remained problematic. The current paradigm for the evolution of the Moon as a planetary body is dominated by the concept of a primordial global lunar magma ocean (LMO) in which the outer ~500 km of the Moon was completely molten due to the high temperatures associated with the Moon's formation [1,2]. As the LMO cooled and crystallized, the Moon became chemically differentiated and a stratified mantle and crust formed, with dense mafic phases settling to the base of the LMO, the lighter plagioclase floating to the surface to form an anorthositic crust, and the final, incompatible trace-element-rich liquid (urKREEP) sandwiched between the two [3]. Since the hypothesized urKREEP source region is the last part of the magma ocean to crystallize, a closure age for this reservoir should provide a constraint for the duration of the lunar magma ocean. Estimates based on Rb-Sr [4,5,6,7] or Sm-Nd model ages [8,9] as well as the short-lived ¹⁸²Hf-¹⁸²W [10] and ¹⁴⁶Sm-¹⁴²Nd [11] chronometers for the crystallization age of the LMO range from as early as 30 Ma after CAIs to as late as 4.25 Ga (~300 Ma after CAIs).

Since Lu/Hf is more highly fractionated than Sm/Nd during silicate differentiation [12], this system can potentially distinguish planetary magmatic processes with greater sensitivity. Prior Lu-Hf studies of lunar materials focused on the younger mare basalts (3.2-3.9 Ga) and elucidated the history of lunar volcanism and mantle source regions [13,14,15,16]. These studies found a wide range of highly positive ϵ_{Hf} values (ranging from +5 to +55) indicating that the basalts were formed from re-melting of mantle sources which had experienced incompatible trace element depletion early in the Moon's history. Based on these data, it was expected that either crustal highland rocks or KREEP-rich rocks would have negative ϵ_{Hf} values, representing an enriched crust complementary to the depleted mantle. Presently, Lu-Hf data are extremely scarce for highland rocks, with one abstract [17] reporting positive ϵ_{Hf} values for Mg-suite and ferroan anorthositic rocks, which is contrary to what is expected. The positive ϵ_{Hf} values suggest that these highland rocks also originated from a depleted source, calling into question the lunar magma ocean (LMO) hy-

pothesis as it is currently understood. An enriched source region (associated with the primary anorthositic crust or with ur-KREEP) must exist but has yet to be documented. This study presents the first isotopic identification of an enriched source on the Moon complementary to the highly depleted mantle source region of mare basalts.

Samples: Zircon is an especially valuable mineral for these studies due to its ability to resist resetting of the U-Pb isotope system in the heavy impact environment of the Moon [18]. Also, the original Hf isotope ratios are well-preserved in zircons because of the extremely low Lu/Hf ratio and the slow diffusion of Hf⁴⁺ in zircons

Over 120 zircons have been isolated from 4 samples (15 g each) of soil and saw cuttings from the Apollo 14 landing site, 80 of which have been analyzed for Lu-Hf isotopes, U-Pb ages and Ti/REE concentrations. Rocks from the Apollo 14 site are dominated by the incompatible element-enriched KREEP component and are high in zirconium content. Three of the samples obtained are saw cuttings from clast-rich polymict breccias (14304, 14305 and 14321), all of which are known to be rich in zircons [19, 20] and which consist of various lithic and single crystal fragments, including basalt clasts, troctolites, anorthosites, granophyres and microbreccia. The fourth sample is an Apollo 14 soil (14163).

Zircons were isolated by heavy-liquid mineral separation techniques followed by hand-picking facilitated by use of UV fluorescence. Because the zircons are found as loose grains in the sample, it is not possible to identify which rocks or clasts are parental to each zircon. All zircons were extensively imaged before and after the different analyses using backscattered electrons and cathodoluminescence to determine zoning and proper location of analysis spots.

Analytical technique: U-Pb ages were obtained using the Cameca 1270 ion microprobe at UCLA and the SHRIMP I ion microprobe at ANU. REE and Ti concentrations were determined using the Cameca 1270 ion microprobe at UCLA. Lu and Hf isotope analyses were undertaken using laser ablation MC-ICPMS according to the techniques described in [21]. The laser ablation spot size was either 60 or 80 μm and with typically sub-epsilon precision being obtained. Correction of isobaric interferences via peak stripping follows the technique used by Harrison *et al.* (2005).

Results and discussion: The Apollo 14 zircons show ages ranging from 3.9 Ga to 4.4 Ga (Fig. 1), consistent with previous studies of Apollo 14 zircons [19, 20] found in situ in association with lunar granophyre fragments. The negative ϵ_{Hf} values determined for some of the Apollo 14 zircons from this study imply that they may be associated with KREEPy materials and indicates that KREEP magmatism as well as formation of granitic rocks [20] was ongoing for a prolonged period of time early in the Moon's history. Crystallization temperatures (Fig. 2) inferred from Ti concentrations [22] range from 880°C to 1180°C, with a mean of 1015°C. This is approximately 300°C higher than the 680°C peak in crystallization temperature of terrestrial Hadean zircons, reflecting the dry and reducing condition of lunar magmas.

Lu-Hf isotopes: The ^{176}Lu isotope data reveal ϵ_{Hf} values ranging from a low of -7 to a high of +4. These data represent the least radiogenic Hf data obtained thus far in lunar materials (compare to $\epsilon_{\text{Hf}} = -1.53$ for Apollo 16 KREEP-rich basalt 65015,190 [15] and $\epsilon_{\text{Hf}} = -1.3$ for high-Al basalt 14053 [17]), implying that the parental magma of some of the zircons was derived from partial melting of an ancient, enriched lunar mantle or crustal reservoir. These zircons represent the first identified samples derived from an early enriched source on the Moon.

Although the long half-life of ^{176}Lu (~37 Ga) does not allow a precise determination of the closure age of the KREEP source region, coupling an estimated Lu/Hf ratio of the ITE-enriched urKREEP with the ϵ_{Hf} vs age array determined by the zircon data can provide upper and lower limits for this age. A preliminary analysis of the least radiogenic group of zircons defines a slope consistent with a Lu/Hf of 0.46 to 0.68 \times CI and a closure age of 4.55 Ga. A best estimate of the Lu/Hf ratio of the KREEP source based upon the average composition of the most concentrated "high-K" variety of KREEP [23] is 0.64 \times CI. A KREEP source region closure age of 4.50 Ga would require a Lu/Hf = 0.083 (0.37 \times CI), much lower than estimated for KREEP. Additionally, the lowest allowable ϵ_{Hf} limit (corresponding to Lu/Hf = 0) requires a closure age no younger than 4.4 Ga. These data are consistent with closure of the KREEP source region within 60 million years of formation of the solar system.

References: [1] Wood J.A. et al. (1970) *Science* 167, 602-604. [2] Warren P.H. (1985) *Ann. Rev. Earth Planet. Sci.*, 13, 201-240. [3] Warren P.H. and Wasson J.T. (1979) *Rev. Geophys. Space Phys.*, 17, 73-88. [4] Papanastassiou D.A. et al. (1970) *EPSL*, 8, 1-19. [5] Nyquist, L.E. (1977) *Phys. Chem. Earth*, 10, 103-142. [6] Carlson R.W. and Lugmair G.W. (1988) *EPSL*, 90, 119-130. [7] Palme H. (1977) *GCA*,

41, 1791-1801. [8] Lugmair G.W. and Carlson R.W. (1978) *LPS IX*, 689. [9] Carlson R.W. and Lugmair G.W. (1979) *EPSL*, 45, 123-132. [10] Kleine T. et al. (2005) *Nature*, 418, 310, 1671-1674 [11] Wadhwa M. pers. comm. (2006) [12] Patchett P.J. (1983) *GCA*, 47, 81-91. [13] Patchett P.J. and Tatsumoto M. (1981) *LPS XII LPS*, 819. [14] Unruh D M et al. (1982) *LPS XIII*, 815. [15] Unruh D.M. and Tatsumoto M. (1984) *LPS XV*, 876. [16] Beard B.L. et al. (1998) *GCA*, 62, 525-544. [17] Lee D.-C. et al. (2000) *LPS XXXI* Abstract 1288. [18] Amelin Y. et al. (2000) *GCA*, 64, 4205-4225 [19] Meyer C. et al. (1989) *LPS XX*, 692. [20] Meyer C. et al. (1996) *MAPS*, 31, 370-387. [21] Harrison T.M. et al. (2005) *Science*, 310, 1947-1950. [22] Watson E.B. and Harrison T.M. (2005) *Science*, 308, 841-844. [23] Warren P.H. (1989) *Workshop on Moon in Transition*, 149-153.

Acknowledgements: We thank NASA and CAPTEM for making the lunar samples available for this study. We also thank Axel Schmitt, Peter Holden, Trevor Ireland, and Les Kinsley for laboratory assistance; and Paul Warren for helpful discussions.

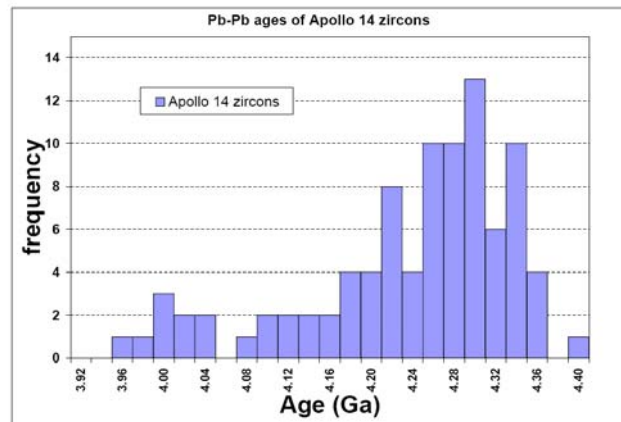


Fig. 1: Pb-Pb ages of Apollo 14 zircons analyzed in this study range from 3.96 to 4.41 Ga.

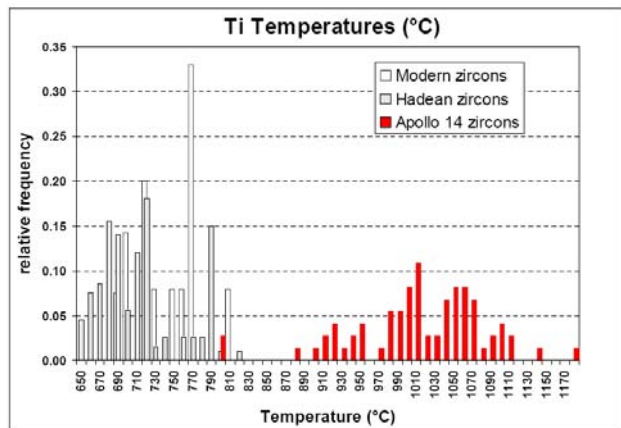


Fig. 2: Crystallization temperatures determined from Ti concentrations. Apollo 14 zircons compared to terrestrial zircons.

THE TYPE Ia SUPERNOVA AS A KEY TO ORIGIN OF THE SOLAR SYSTEM. G. K. Ustinova, Vernadsky Institute of Geochemistry and Analytical Chemistry, Russian Academy of Sciences, Moscow V-334, 119991 Russia; e-mail: ustinova@dubna.net.ru

Introduction: The Solar System is a valuable astrophysical laboratory because it represents the final results of wide-ranging nebular processes leading to formation of stars with planetary systems. The main and the most important link of such investigations is the isotopic and elemental composition of the primordial matter. The contemporary level of knowledge is based on the conception that the primordial matter originated from the matter of the giant molecular gas-dust nebula, which was distributed homogeneously with the products of the nucleosynthesis of about ten of supernovae during ~ 10 Ma of the nebula existence before turbulent dissipation (e.g. [1]). However, the numerous isotopic anomalies in meteorites, which are conditioned by the decay of some extinct radionuclides, suggest that, at least, one of the supernovae had been exploded shortly before the collapse of the protosolar nebula [2] The matter of the last supernova cannot yet be mixed evenly with the matter of the molecular cloud: it rather flowed round, surrounding the cloud gradually (e.g. [3]). The intervals of generation of the short-lived extinct radionuclides of ^{41}Ca , ^{26}Al and ^{53}Mn in the calcium and aluminium rich inclusions (CAI) of carbonaceous chondrites testify to the last supernova explosion ≤ 1 Ma before the formation of the solid phases of the primordial matter [4-7]. The absence of heavier extinct radionuclides (the products of r -process) with the similar intervals of generation in CAI indicates that the last supernova was the Type Ia Supernova (Sn Ia), the so-called carbon-detonation supernova, which could not survive the carbon explosive burning and was fully disrupted [5,6,8].

The Type Ia Supernovae: Sne Ia turned out to be the ideal objects for estimating the Hubble constant and, so, the properties of these supernovae are being studied intensively over last years (e.g., [9,10]). For the most part, Sne Ia are the explosions of white dwarfs, consisting of carbon and oxygen, that have approached the Chandrasekhar mass, $M_{\text{Chan}} \approx 1.39$ solar masses (M_{\odot}). At the explosive burning of carbon and oxygen, releasing the energy of $\sim 10^{51}$ erg, all the intermediate-mass elements like Mg, Si, S, Ca are synthesized, but the doubly-magic nucleus ^{56}Ni is produced with the highest probability. During 6.1 days ^{56}Ni decays to ^{56}Co , and then the latter decays to ^{56}Fe over 77 days. Depending on the initial C/O composition of white dwarfs, the Sn Ia explosion produces 0.4-0.6 M_{\odot} of ^{56}Fe , substantial amounts of the intermediate-mass elements, and, besides, some unburned

amounts of C+O can be ejected [11,12].

The peculiarities of the Sn Ia may specify the uniqueness of the Solar System among the other planetary systems being forecasted.

Heterogeneity of accretion: The current concept is that the chemical and isotopic composition of the primordial matter was homogeneous and similar to the contemporary solar one [13] in many respects. It is based on the supposed absence of essential fractionation at the collapse stage of the molecular gas-dust clouds during the formation of the planetary systems (e.g., [14]). However, Sn Ia explosion just before the origin of the Solar System, especially, if its matter surrounded the collapsing nebula, led to rather a heterogeneous accretion: the specific matter of Sn Ia (e.g., the ratio of Fe to Si-Ca is higher by a factor of about 2-3 than in the solar composition [12]) accreted mainly at the concluding stage of formation of the Solar System, enriching the latter with iron, intermediate elements, as well as, with unburned C and O. It looks tempting that just the enrichment of the upper mantle of the Earth with the unburned C and O has provided the basis for some pre-biological background and the subsequent origin of life on the Earth.

Separation by turbulence: Turbulence in the collapsing protosolar nebula ensured the further large-scale chemical separation of the matter. In a sense, turbulence in the nebula is the formation and dissipation of vortices of various scales. Due to the magnetic hydrodynamic (MGD) mechanism of separation, the vortex in the nebula pulls in the new incoming nuclei (e.g., the Sn Ia products) to its vertex (i.e. to its center): the large nuclei (e.g., Fe) before the small ones (e.g., Si-Ca). In other words, there is separation of matter with some time lag (just as in the hydrodynamics such an effect is conditioned, eventually, by the Bernoulli law (see, e.g., [15,16]). But, such an effect is just the cause of the matter separation at the very initial stage of turbulence in the collapsing protosolar nebula in the conditions of the incoming specific matter of the Sn Ia due to the specific mechanism of its acceleration in the explosive shock wave (the shock-wave acceleration of particles forms their very rigid power-law energy spectrum enriched with heavier nuclei [17,18].

Drafts of scenarios: Thus, the Sn Ia explosion opens, apparently, a clue to the origin of the celestial bodies, and primarily:

Iron meteorites. The large quantity of synthesized and accelerated iron nuclei were among the first ones

that penetrated into the collapsing protosolar nebula and, being captured by supersonic turbulence, they created some iron-rich regions of various scale, so that the further condensation and accumulation in those regions formed the iron planetesimals and iron parent bodies. In other words, it means that the metal-silicate separation could occur before condensation.

Earth group planets. In some cases of especially huge vortices the captured iron underlaid the metallic core embryos of some planets, which further were built up due to magmatic differentiation. The intermediate and light nuclei of the Sn Ia explosion also reached the accreting system and rather later were captured gradually by the especially huge vortices, which still were not dissipated. Because of the turbulence drawing into the central plane of the accretion disk, the intermediate-mass and light elements had played the key role in formation of the earth group planets under the reducing conditions being typical for the corresponding heliocentric distances. In particular, the extinct radionuclides (especially, ^{26}Al) were among the Sn Ia products, as well as among the products of spallation reactions induced by the shock-wave accelerated nuclear-active particles (Ustinova 2002c), so, their decay provided the further thermal evolution of the planets and some (differentiated) meteorites.

Stony meteorites. When practically all the injected iron was caught by the turbulence, the new developed vortices captured the intermediate-mass explosion products. Depending on the distance from the protosun, and, therefore, from the different pressure-temperature (PT-) conditions of condensation, the different types of stony bodies of various scale were created, whose accumulation led later to the formation of stony planetesimals and the parent bodies of stony meteorites of different types. Certainly, all the possible cases of the blended matter could occur.

Carbonaceous chondrites. The most part of the unburned C and O of the exploded Sn Ia was accreted at the conclusive stage of accretion in the various conditions of low temperatures and free gravitation that provided the formation of carbonaceous chondrites of different types. Clearly, that the famous oxygen anomaly, existence of pure ^{16}O in carbonaceous chondrites [19] is natural.

Giant planets were apparently formed by the giant vortices in the main matter of the protosolar molecular nebula at the distances which had not been reached by the exploded matter of the Sn Ia.

Of course, the real processes are much more complex, and the presented simplified drafts give us only the frame descriptions of future accretion models, which demand the further thorough development by

the specialists in the different fields of science and especially, perhaps, in plasma physics [20]

Conclusion: The obtained sequence of formation of the Solar System bodies is consistent with the recent remarkable finding in the Hf-W chronometry of meteorites [21-23] that the core formation in the parent asteroids of iron meteorites predates the accretion of the chondrite parent bodies. It is in contradiction with the current accretion models based on the conception that the chondrites represent the precursor material, from which asteroids accreted and then differentiated. Therefore, a new accretion model is really required. It must be a MGD model, in which the specific matter of the Sn Ia, surrounding the protosolar nebula, is considered as a boundary condition instead of the interstellar medium as in the case of the models of other possible planetary systems [20]. Initial MGD separation of matter and its fractionation during shock wave acceleration [17] must be taken into account too.

References: [1] Larson R. B. (1981). *Mon. Not. R. Astr. Soc.* 194, 809-826. [2] Wasserburg G. J. and Papanastassiou D. A. (1982) In: Barnes, C. A., Clayton D. D., Schramm D. N. (Eds.), *Essays in Nuclear Astrophysics*, Cambridge Univ. Press, Cambridge, chap. 6. [3] Schramm D. N. (1978). In: Gehrels T. (Ed.) *Protostars and Planets*, Univ. Arizona Press, Tucson, pp. 384-398. [4] Srinivasan G. et al. (1996) *GCA*, 60, 1823-1835. [5] Ustinova G. K. (2002). *Doklady (Transactions) RAS* 382, 242-245. [6] Ustinova G. K. (2002). *LPS XXXIII*, Abstract #1015. [7] Cameron A.G.W. (2003). *LPS XXXIV*, Abstract #1083. [8] Ustinova G. K. (2002). *Geochemistry International* 40, 827-842. [9] Branch D. (1998). *Ann. Rev. Astron. Astrophys.* 36, 17-55. [10] Branch D. (2003). *Science* 299, 53-54. [11] Gamezo V. N. et al. (2003). *Science* 299, 77-81. [12] Thielemann F.-K. et al. (2005). *Proc. 22nd Int. Nucl. Phys. Conf.*, Göteborg, 2004, Elsevier, Amsterdam, pt.1, pp. 301-328. [13] Gressve N. and Sauval A. J. (1998). *Space Sci. Rev.* 85, 161-174. [14] Cassen P., Shu F. H., and Terebey S. (1985). In: Black D. C., Matthews M. S. (Eds.) *Protostar and Planets II*, Univ. Arizona Press, Tucson, pp. 448-483. [15] Landau L. D. and Lifshitz E. M. (1986). *Theoretical Physics. Vol. VI. Hydrodynamics*. Nauka. Moscow. [16] Feynman R.P., Leighton R.B., and Sands M. (1964). *The Feynman Lectures on Physics. Vol. 2. Physics of Continua*. Addison-Wesley Publishing Company, Inc. [17] Eichler D. and Haebach K. (1981). *Phys. Rev. Lett.* 47, 1560-1563. [18] Ellison D. C. and Eichler D. (1984). *Astrophys. J.* 256, 691-701. [19] Clayton R. N., Grossman L. and Mayeda T. K. (1973). *Science* 182, 485-488. [20] Ustinova G. K. (2004) *LPS XXXV*, Abstract #1195. [21] Yin Q. Z. et al. (2002). *Nature* 418, 949-952. [22] Kleine T. et al. (2002). *Nature*. 418, 952-955. [23] Kleine T. et al. (2005). *GCA* 69, 5805-5818.

BULK EARTH COMPOSITIONAL MODELS ARE CONSISTENT WITH THE PRESENCE OF POTASSIUM IN EARTH'S CORE. W. van Westrenen¹ and V. Rama Murthy², ¹Faculty of Earth and Life Sciences, Vrije Universiteit Amsterdam, De Boelelaan 1085, 1081 HV Amsterdam, The Netherlands. wim.van.westrenen@falw.vu.nl, ²Institute of Meteoritics, 1 University of New Mexico, MSC03-2050, Albuquerque, NM 87131, USA. vrmurthy@unm.edu.

Introduction: Constraining the distribution of radioactive potassium-40 as a heat source in planetary interiors is crucial for the development of accurate models for the thermal evolution of differentiated bodies. We show that geo/cosmochemical models for the composition of the Bulk Earth and core are consistent with results from high-pressure experiments and thermal evolution models in allowing for the presence of up to 250 ppm K in Earth's core, contrary to recent claims in the literature.

Background: A growing body of experimental evidence suggests that significant amounts of potassium can be incorporated into sulphur-bearing iron melts at relatively low pressure (e.g. [1], Fig. 1.), and in sulphur-free iron melts at high pressure (e.g. [3,4]).

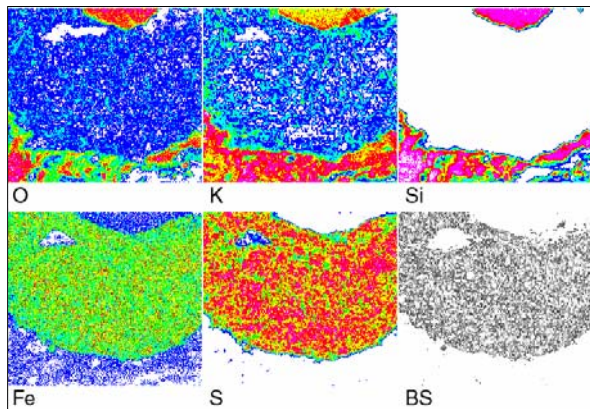


Figure 1: X-ray element and back-scatter electron maps of metal-silicate partitioning experiment (1873 K, 2 GPa) from [1], showing abundant K and O in Fe-S liquid. Element distributions shown for O, K, Si, Fe and S, and back-scatter electron image (marked BS) shown in lower right corner. Red denotes high concentrations, blue low concentrations, and colourless denotes the element is not present above detection limit. Dimensions of each panel: 150 x 150 microns.

For the Earth, predicted core K concentrations of a few hundred ppm are consistent with core K levels invoked by recent core/mantle thermal evolution studies (e.g. [5,7,8]). In spite of these studies, the notion of core K is questioned in the context of geo/cosmochemical models for the composition of the bulk silicate Earth (BSE) and Earth's core (e.g. [2,9-11]). Arguments against the presence of potassium in

the core are based on: (1) Trends in the elemental composition of the bulk silicate Earth (BSE) compared to the composition of CI carbonaceous chondrite (CC) as a function of element condensation temperatures [2,9], (2) Systematics of K/U versus Rb/Sr concentration ratios in BSE and chondrites [10], and (3) The mantle abundance of Ca relative to other refractory lithophile elements on the presumption that K entry into the core also extracts Ca [2,11]. Below we show that none of these arguments are valid, and that Bulk Earth compositional models can easily accommodate up to 250 ppm K in Earth's core.

Discussion: Popular models for the chemical composition of the Earth rely on a comparison between BSE and chondritic meteorite compositions (e.g. [2,9]). With the exception of refractory, non-volatile elements all elements, including potassium, are less abundant in BSE than in C1 chondrites. The C1-normalised BSE abundances of many lithophile elements (e.g. Si, Li, Na, K) appear to vary systematically with their condensation temperatures: the lower the condensation temperature, the lower the C1-normalised BSE abundance (Fig. 2).

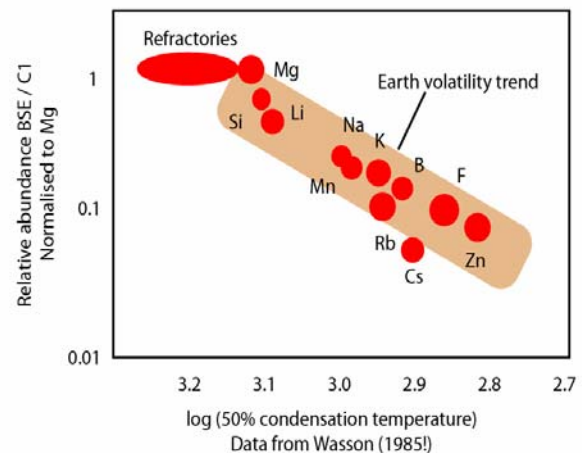


Figure 2: C1-normalised BSE concentrations versus condensation temperature for selected elements (after [2]). Shaded area known as 'Earth volatility trend'.

The first argument against K in Earth's core is the fact that K's behaviour appears fully consistent with that of other lithophile, volatile elements, in that its C1-normalised BSE concentration plots along the broadly defined 'Earth volatility trend' (Fig. 2, after

[2]). This argument relies on literature compilations of meteorite compositions and condensation temperatures that are approximately 20 years old [12,13]. A recent compilation of C1 compositions and condensation temperature calculations by Lodders [6] shows that a much more tightly constrained volatility trend can be identified for Earth (Fig. 3). The C1-normalized K concentration of the BSE from [2] clearly falls below this trend: This is not consistent with K depletion in BSE being the result of K volatility only. To return K to its place on the volatility trend, 264 ppm K would need to be added to Earth's core. This simple exercise shows that volatility trends cannot be used to advocate the absence of K (or other elements plotted in Figs. 2 and 3) from Earth's core.

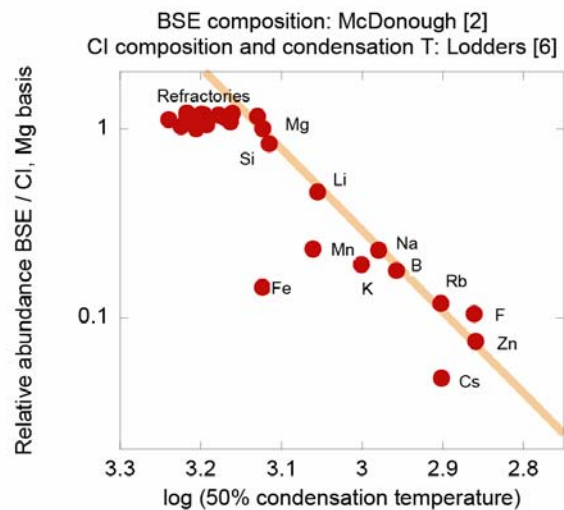


Figure 3: C1-normalised BSE concentrations versus condensation temperature for selected elements using [2,6]. Shaded line shows alternative, tightly constrained volatility trend for Earth.

The second argument against core K relies on a supposedly linear correlation for chondrites and BSE between K/U and Rb/Sr ratios [10]. Assuming U, Rb and Sr are absent from the core (consistent with Figs. 2 and 3), it is argued that any core K would destroy this correlation. The correlation is based on a compilation of meteorite compositions which does not provide any estimates of uncertainties in concentrations or ratios [12]. Lodders and Fegley [15] provide a more recent compilation, and the Tagish Lake meteorite fall provides an additional chondrite class for which compositional measurements, including errors, are available for comparison. Fig. 4 shows that chondrite trends of K/U versus Rb/Sr are not as linear as previously claimed. Adding 250 ppm K to Earth's core is fully consistent with data for other chondrites. Furthermore, assuming the error bars on the Tagish Lake and C1 data are rep-

resentative, it appears that this type of plot cannot be used to constrain Earth core concentrations of any of the four elements involved.

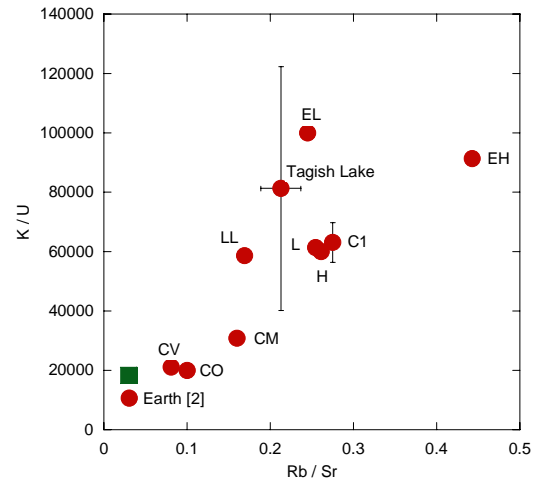


Figure 4: K / U versus Rb / Sr in chondrites [6,15], Earth [2] (circles), and Earth assuming 250 ppm core K in the absence of core U, Rb and Sr (square).

Finally, McDonough and others [2,11] argue that Ca enters metallic liquid along with K [14], so that K extraction into the core leads to subchondritic refractory element ratios such as Ca/Al, Ca/Sc etc., contrary to observation. This argument is misleading in that a simple calculation using the Ca partitioning values of [14] demonstrates that the effect of Ca extraction would be small and entirely within the 10% error of the estimated BSE Ca abundance.

Conclusions: There is no conflict or inconsistency between geo/cosmochemical Bulk Earth models and the presence of significant amounts of K in Earth's core indicated by recent experimental data.

References: [1] Rama Murthy V. et al. (2003) *Nature*, 423, 163-165. [2] McDonough W. F. (2003) *Treat. Geochem.*, 2.18. [3] Lee K. K. M. and Jeanloz R. (2003) *GRL*, 30, 2212. [4] Hirao N. et al. (2006) *GRL*, 33, L08303. [5] Nimmo F. et al. (2004) *GJI*, 156, 363-376. [6] Lodders K. (2003) *Astrophys. J.*, 591, 1220-1247. [7] Nakagawa T. and Tackley P. J. (2005) *G³*, 6, Q08003. [8] Costin S. O. and Butler S. L. (2006) *PEPI*, 157, 55-71. [9] Palme H. and O'Neill H. St. C. (2003) *Treat. Geochem.*, 2.01. [10] Halliday A. N. (2003) *Treat. Geochem.*, 1.20. [11] Keshav S. et al. (2005) *LPS XXXVI*, Abstract #2016. [12] Wasson J. T. and Kallemeyn G. J. (1988) *Phil. Trans. Royal Soc.*, A325, 535-544. [13] Wasson J. T. (1985) *Meteorites - Their record of early solar-system history*, Freeman. [14] Gessmann C. K. and Wood B. J. (2002) *EPSL*, 200, 63-78. [15] Lodders K. and Fegley B. (1998) *The planetary scientist's companion*, Oxford.

Osmium Isotope and Highly Siderophile Element Abundance Constraints on the Nature of the Late Accretionary Histories of the Earth, Moon and Mars. Richard J. Walker - Department of Geology, University of Maryland, College Park, MD 20742, USA (rjwalker@geol.umd.edu).

Introduction: The highly siderophile elements (HSE) include Re, Os, Ir, Ru, Pt and Pd. These elements are initially nearly-quantitatively stripped from planetary silicate mantles during core segregation. They then may be re-enriched in mantles via continued accretion *sans* continued core segregation [1]. This suite of elements and its included long-lived radiogenic isotopes systems ($^{187}\text{Re} \rightarrow ^{187}\text{Os}$; $^{190}\text{Pt} \rightarrow ^{186}\text{Os}$) can potentially be used to “fingerprint” the characteristics of late accreted materials. The fingerprints may ultimately be useful to constrain the prior nebular history of the dominant late accreted materials, and to compare the proportion and genesis of late accretionary materials added to the inner planets.

The past ten years have seen considerable accumulation of isotopic and compositional data for HSE present in the Earth’s mantle, lunar mantle and impact melt breccias, and the Martian mantle. Here I review some of these data and consider the broader implications of the compiled data.

Earth. Of perhaps greatest importance to humans is the late accretionary history of the Earth. In addition to the fact that you can still get hit on the head by late accreted materials, it has also been widely suggested that late additions to Earth could have provided the planet with much of its water, with organic matter, and even life. Studies of the Os isotopic compositions of terrestrial peridotites that have been long isolated from convection in the upper mantle (e.g. ancient subcontinental lithospheric mantle) led to the conclusion that: a) important constraints can be placed on the Os isotopic composition of the Primitive Upper Mantle (mantle unmodified by melt depletion or enrichment), and 2) the inferred $^{187}\text{Os}/^{188}\text{Os}$ of Earth’s dominant late accreted materials matches that of enstatite/ordinary chondrites, not the more volatile rich carbonaceous chondrites [2].

Recent attempts to constrain the absolute and relative HSE budget of the PUM have led to recognition that there are some discrepancies between PUM and chondrites. For various suites of peridotites (including continental mantle, orogenic lherzolites and abyssal peridotites), HSE were recently correlated with melt depletion/enrichment indicators and extrapolated to an estimate of the PUM [3]. For most HSE, abundances in PUM are similar to earlier estimates. However, estimates of Ru/Ir and Pd/Ir derived from most suites indicates modestly suprachondritic compositions for average PUM. This has been observed by other groups as well [4-5], although the effects of melt depletion can now be

discounted. Thus, although HSE in the terrestrial PUM can be placed in a broad “chondritic” family, it is not a perfect match to any one chondrite group that exists in our collections. This can be interpreted in one of several ways. First, the dominant late accreted materials may have had a somewhat different nebular history compared to the chondrites in our collections. This would not be surprising. Nebular, and perhaps subsequent processing on parent bodies has been shown to result in considerable fractionation of HSE [6]. Second, the deviation from chondritic ratios could be an indication that processes other than, or in addition to late accretion controlled HSE abundances in the mantle. For example, many workers have experimentally explored the possibility that the comparatively high abundances of HSE in the mantle are a result of relatively low metal-silicate bulk partitioning at the base of a deep magma ocean [7]. I consider this an unlikely explanation for Os isotopic systematics, given the close adherence of $^{187}\text{Os}/^{188}\text{Os}$ and $^{186}\text{Os}/^{188}\text{Os}$ to chondritic (which allows us to constrain Re/Os and Pt/Os in the PUM better than any other HSE ratios). Retention of precisely chondritic Pt/Re/Os is an unlikely result of metal-silicate partitioning. Nonetheless, this possibility begs future experimental consideration. Also, retention of excess Ru and Pd in the silicate Earth following metal segregation, relative to other HSE, could result in suprachondritic ratios involving these elements, allowing the possibility of a hybrid model for generating HSE abundances. Finally, it may be that mantle processes (melt removal & refertilization, crustal recycling) have complicated the HSE budget of the mantle beyond our current capability to deconvolute them and obtain an accurate estimate of the PUM.

Moon. We recently completed a study of the Os isotopic and HSE concentration systematics of lunar picritic orange and green glasses with the intent of constraining Os concentration in the lunar mantle sources of these relatively high MgO melts [8]. We discovered that residues of leached glass spherules contained more radiogenic Os than the leachates, but lower Os abundances, suggesting the presence of at least two Os (and likely other HSE) components. The presumed radiogenic indigenous component has much lower Os and HSE concentrations than had been previously presumed for lunar glasses. This may be a reflection of the mantle sources of the glasses containing low concentrations of these elements.

Relative to terrestrial rocks with comparable MgO contents (**Fig. 1**), the lunar mantle sources of the

orange and green glasses were depleted in the HSE by at least a factor of 20. This observation may indicate that the lunar mantle did not receive a late accretionary component like that suggested to explain the HSE budget of Earth's mantle. The "missing" HSE could reside in the lunar crust, which is both ancient and thick, and may have protected the lunar mantle from much of the putative late influx of material. Alternately, the missing HSE could have been extracted into a small lunar core at the time of its formation, or may even continue to reside in the lunar mantle in residual metallic iron. The latter two hypotheses can be tested, because metal would likely lead to strong fractionation of Re from Os in the silicate mantle. This is because metal has less affinity for Re than Os. Consequently, other materials derived from the lunar mantle, such as basalts, would likely show supra-chondritic Os isotopic compositions at the time of their formation, if metal was responsible for the apparent depletion of HSE in the lunar mantle. Preliminary results show that this is not the case but much additional work will be required.

Potentially direct information regarding the chemical nature of late accreted materials to the Earth-Moon system can be obtained by examining the HSE contained in lunar impact-melt rocks. The HSE contained in melt rocks were largely added to the Moon during the period of time from the origin of the lunar highlands crust (4.4-4.5 Ga) to the end of the late bombardment period (~3.9 Ga). Removal of the effects of indigenous contributions from the HSE of impact-melt rocks is critical to accurately fingerprinting the HSE of the impactors. Considerable HSE and Os isotopic data now exist for A17 and A14 impact melt rocks. Our results [9], together with those of Norman et al. [10] suggest that there is some variability in the HSE systematics of A17 melt rocks. For some rocks there is an indication of resolvable indigenous Ru and Pd. Of note, and relevant to the discussion of the terrestrial PUM above, indigenous corrected values of Ru/Ir for some breccias plot above the highest end of the range for ordinary and enstatite chondrites, and in some cases matches that of the PUM estimate. As with the estimate for the terrestrial PUM, however, results must be further scrutinized. In addition to necessary corrections for indigenous components, possible HSE fractionation resulting from volatility or other processes may have complicated the signal injected by the impactors. Further examination of HSE abundances in pristine lunar rocks must be conducted.

Mars. Re-Os studies of SNC meteorites indicate that the Martian mantle evolved with a dominantly chondritic Re/Os [11]. As with the terrestrial mantle, this is most easily explained via the addition of a late veneer with chondritic Re/Os subsequent to core for-

mation. In addition, most of the meteorites have Os concentrations broadly consistent with derivation from mantle sources bearing Os concentrations similar to those present in the terrestrial upper mantle (**Fig. 1**). This may suggest a veneer of approximately the same proportion as was added to Earth. Of note, the extremely low concentrations of Re and Os present in 84001 may reflect derivation from a mantle reservoir that had not yet accumulated much of its late veneer prior to the very early formation age of the meteorite.

References. [1] Chou (1978) *Proc. 9th Lunar Planet. Sci. Conf.*, 219-230. [2] Meisel et al. (2001) *Geochim. Cosmochim Acta* **65**, 1311. [3] Becker et al. (2006) *Geochim. Cosmochim Acta* **70**, 4528. [4] Pattou et al. (1996) *Nature* **379**, 712. [5] Schmidt (2004) *Met. Planet. Sci.* **39**, 1995. [6] Horan et al. (2003) *Chem. Geol.* **196**, 5. [7] Drake (2000) *Geochim. Cosmochim Acta* **64**, 2363. [8] Walker et al. (2004) *EPSL* **224**, 399. [9] Puchtel et al (2006) *LPSC XXXVII*, Abst. #1428. [10] Norman et al. (2002) *EPSL* **202**, 217. [11] Brandon et al. (2000) *Geochim. Cosmochim Acta* **64**, 4083.

Acknowledgements. This work was supported by NASA grants NNG04GJ49A and NNG04GK52G, and NSF grant EAR0207107.

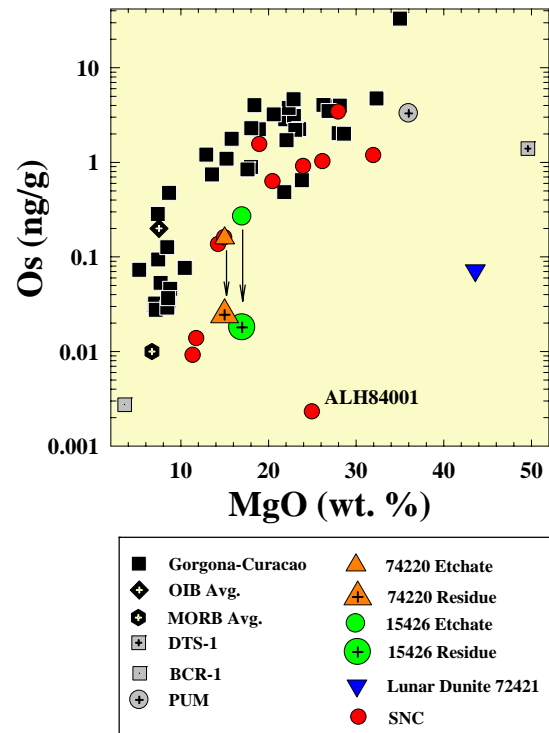


Fig. 1. MgO vs. Os for typical terrestrial rocks, lunar orange and green glasses, and Martian SNC meteorites. Concentrations of etchates and residues of green glass 15426,164 (>200 μm) and orange glass 74220 (74-150 μm) are shown. The Os concentrations of the indigenous components in the lunar glasses (residues) are considerably less than the concentrations in the bulk glasses. SNC meteorites plot at the lower end of the terrestrial array, with ALH84001 plotting well below the Martian trend. Most data from [8 & 11].

Exploring the Geochemical Consequences of Magma Ocean Differentiation M. J. Walter¹

¹Department of Earth Sciences, University of Bristol, Queen's Rd., Bristol BS8 1RJ, U.K.

Introduction: Modern accretion theory depicts a violent early Earth [1], and we expect that impact accretion caused several or many partial or wholesale melting events. Transient magma ocean stages would invariably have led to intervals of metal segregation to form the core and crystallization and melt expulsion in the silicate, and these events created gross chemical heterogeneity in the very early Earth. It is evident that modern Earth retains a partially molten metallic core, but whether any permanent early differentiation in the silicate mantle has survived Earth's convection engine and remains traceable in the modern geochemical record is debatable. Accretion is an inherently stochastic process so a single model for differentiation is of little predictive value. Here, we will present a set of general petrologic and geochemical models to explore how processes such as fractional crystallization and partial melt expulsion might have left imprints on the modern geochemical record.

What kind of models? One can make many assumptions about how a magma ocean might crystallize. What is clear is that a magma ocean geotherm will be shallower than the liquidus of mantle silicate. That is, the magma ocean would crystallize from the bottom up [2]. It is unclear how much crystallization might also occur near the surface. It all depends on whether an insulating atmosphere is present (e.g. silicate vapor, water, methane) [3].

Physical models show how it is inappropriate to use a crustal magma chamber as a magma ocean analog [4, 5]. Ultramafic liquid at magma ocean temperatures has very low viscosity, and precipitation of silicate crystals is more closely analogous to formation of ice crystals in the atmosphere. Under such conditions crystal settling may not occur due to the highly turbulent nature of convection currents. It all depends on crystal nucleation and growth rates and relative viscosities of crystals and melt; things we don't know much about [5]. Fractional crystallization may have occurred in the deep mantle. At some point a partially crystallized magma achieves a high-enough viscosity for crystal segregation and melt expulsion to occur; this value may be close to 2/3 crystallized for the mantle. So opportunity clearly existed for fractional crystallization at transition zone and upper mantle depths. It is also very likely that once the magma ocean crystallized to >80%, solid-compaction and melt expulsion (like occurs at ridges today for example) would occur forming a basaltic, picritic or komatiitic protocrust.

The possible existence of such an early protocrust is consistent with recent ¹⁴²Nd isotopic measurements [6].

The depth and maximum pressure of any particular magma ocean being variable, one must explore the entire pressure range of the modern mantle. This is especially true if the final, Moon-forming impact melted the whole planet, a calculated possibility [7]. One must be armed with knowledge of crystallization phase relations and element partition coefficients to fully constrain any model. The phase relations required include crystallization involving Mg- and Ca- silicate perovskite (post-perovskite is irrelevant at liquidus temperatures in the mantle) and ferropericlase at lower mantle pressures, majorite, Ca-Pv, pyroxene and olivine polymorphs at transition zone depths, and olivine, pyroxenes and aluminous phases at shallow levels. There is now a large database with which to accomplish this, but the availability of data diminishes with increasing depth so that modeling crystallization at depths greater than about 700 km is best-guess work.

Deep Mantle Crystallization: Crystallization differentiation involving Mg-perovskite in the lower mantle has long been considered a possibility because the deep mantle is the most likely place to preserve heterogeneity over the timescale of Earth [8]. Although ferropericlase is the liquidus phase at about 650 km, recent experimental evidence indicates that Mg-perovskite will be the liquidus phase at depths greater than ~ 700 km [9]. Furthermore, Ca-perovskite, found only near the solidus at ~ 20 GPa, approaches the liquidus at higher pressures.

Crystallization of Mg-perovskite causes fractionation in many refractory lithophile element (RLE) ratios all of which are within 20% relative of chondritic in primitive mantle [10, 11]. Most notably Mg-Pv increases the Lu/Hf ratio in the melt (residual mantle) and no more than ~5% fractionation is permitted on isotopic grounds (i.e. modern mantle derived magmas form an array of Nd and Hf isotopic compositions that passes through estimates of bulk Earth composition) [10].

Ca-Pv has very high partition coefficients for many RLE [12] and, more notably, fractionates most ratios in the opposite sense to that of Mg-perovskite. That means that a little Ca-Pv in the crystal mix goes a long way in imparting geochemical flavor. For example, models show that at ~15% crystallization of Mg-Pv + 5% CaPv, can be tolerated on isotopic and geochemical grounds [12].

‘Transition-zone’ Crystallization: At transition zone depths, majorite is the liquidus phase. Ca-perovskite is a near-solidus phase near the base of the transition zone. Majorite causes extreme fractionations in many RLE ratios, especially those involving aluminum. Less than 5% fractionation of this phase can be tolerated on the basis of Ca/Al, Al/Ti and Al/Sc ratios is primitive mantle. Further, majorite significantly reduces the Lu/Hf ratio and no more than a few percent fractionation is permitted on isotopic grounds. Crystallization of minor amounts of Ca-Pv at transition zone depths further reduces Lu/Hf and so fractionation of transition zone phases does not appear to have occurred, or if it did, convection has caused rehomogenization.

Upper mantle differentiation: Olivine can float in peridotite melt at pressures above ~ 8 GPa [8]. Can this account for the high Mg/Si ratio in primitive upper mantle peridotites? The answer is apparently no as the amount of crystallization needed would have fractionated the Ni/Co ratio of the upper mantle well away from its near chondritic value. More likely the final stage of magma ocean crystallization involved melt expulsion. One can model this basically as a large partial melting event like at a super mid-ocean ridge or ‘mega’—hotspot. We are currently developing models to determine how much shallow melt extraction and permanent storage of a mafic proto-crust can be tolerated on geochemical and isotopic grounds.

1. Chambers, J.E., (2004), *Earth and Planetary Science Letters*, 223, 241-252.
2. Presnall, D.C., et al., (1998), *Physics of the Earth and Planetary Interiors*, 107, 83-95.
3. Abe, Y., (1997), *Physics of the Earth and Planetary Interiors*, 100, 27-39.
4. Tonks, W.B. and H.J. Melosh, in *Origin of the Earth*, H.E. Newsom and J.H. Jones, Editors. 1990, Oxford University Press: New York. p. 151-174.
5. Solomatov, V.S., in *Origin of the Earth and Moon*, R. Canup and K. Righter, Editors. 2000, The University of Arizona Press: Tucson. p. 323-338.
6. Boyet, M., et al., (2003), *Earth and Planetary Science Letters*, 214, 427-442.
7. Canup, R., (2004), *Icarus*, 168, 433-456.
8. Agee, C.B. and D. Walker, (1988), *Earth and Planetary Science Letters*, 90, 144-156.
9. Ito, E., et al., (2004), *Physics of the Earth and Planetary Interiors*, 143-144, 397-406.
10. Walter, M.J., et al., (2004), *Geochimica et Cosmochimica Acta*.
11. Corgne, A. and B.Wood, (2004), *Geochimica et Cosmochimica Acta*, in press.
12. Hirose, K., et al., (2003), *Physics of Earth and Planetary Interiors*.

SIDEROPHILE ELEMENT IMPLICATIONS FOR THE STYLE OF DIFFERENTIATION OF THE HED PARENT BODY.

Paul H. Warren, Institute of Geophysics, UCLA, Los Angeles, CA 90095-1567, USA

The basaltic (eucrite) component of the principal HED asteroid (Vesta?) is widely assumed to have formed by a single stage of differentiation, i.e., simple partial melting, of the primitive, near-chondritic interior of the asteroid [1]. I have previously noted [2,3] that such a model cannot be reconciled with the very large component of magnesian orthopyroxenite cumulate (diogenite) implied for the eucrite asteroid by regolith breccia samples (howardites) of the same parent asteroid. This argument has never been rebutted, but it has been generally ignored. Here, I discuss another fatal flaw with the canonical one-step partial melting scenario for eucrite petrogenesis.

Among eucrites, the siderophile element W displays a good correlation with incompatible lithophile elements such as La [4]. As noted by Jones [5], this can only mean that no metal was present when silicate differentiation determined the range of eucrite compositions. Yet Vesta is known to possess a large core [6], and HEDs formed at consistently very low oxygen fugacity, so the initial, primitive materials of this asteroid were presumably metal-rich.

Our recent studies of ureilites [6] have provided a clearer picture of the process of core formation within differentiated asteroids. Ureilites are restites from which virtually all trace of basaltic (Al-rich) matter was removed by anatexis – in which sense they should be analogs of the most extreme mantle restites complementary to the eucrites. Many elements (e.g., Au, Ni, As) appear to have been depleted from ureilites as siderophile elements, probably by sequestration into the asteroid's metallic core. Paradoxically, however, the most “noble” or highly siderophile elements (HSE, e.g., Ir and Os) are not as greatly depleted [7].

These ureilite observations suggest that asteroidal core formation tends to proceed in two stages [7]. In the first stage, S-rich metallic liquids separate from the silicate matrix. These S-rich metallic liquids deplete moderately siderophile elements such as Au, Ni, As, much more than “noble” siderophiles such as Ir, because solid FeNi metal is mainly trapped in the matrix, and chalcophile tendency trumps siderophile tendency in determining liquid metal/solid metal partitioning behavior [8]. The important point for present purposes is that the ureilite evidence suggests that the second stage of asteroidal core formation, final removal of all metal, probably requires that melting proceed far beyond the point of total depletion of basaltic (Al-rich) matter from the mantle restites. Ureilites are depleted

in “noble” siderophiles such as Ir to only mild extents (e.g., the average ureilite retains Ir, Os, Re and Ru all at ~ 0.5 times CI levels).

Putting these constraints together, the complete absence of metal from the eucrite source regions [5] leads to a second fatal conundrum for the simple partial-melting petrogenetic scenario for eucrites. The complete removal of metal implies such a high degree of prior differentiation of the source material, by analogy with ureilites [7], that the source should have previously been depleted of all basaltic (Al-rich) matter – in which case it would be hopelessly ill-suited to serve as a mantle source region for eucritic partial melts.

A more plausible scenario is one in which the eucrites represent extruded (and in some cases intruded) residual melts from a very large magma system, i.e., a global “magma ocean” or something close to it [3,6,7].

References: [1] Stolper E. (1977) *GCA* 41, 587. [2] Warren P. H. (1985) *GCA* 49, 577. [3] Warren P. H. (1997) *MAPS* 32, 945. [4] Newsom H. E. and Drake M. J. (1982) *GCA* 46, 2483. [5] Jones J. H. (1993) *EOS* 74, 654. [6] Ruzicka A. et al. (1997) *MAPS* 32, 825. [7] Warren P. H. et al. (2006) *GCA* 70, 2104. [8] Chabot N. L. and Jones J. H. (2003) *MAPS* 38, 1425-1436..

EARTH AFTER THE MOON-FORMING IMPACT. K. J. Zahnle¹ and W. B. Moore², ¹NASA Ames Research Center (Kevin.J.Zahnle@NASA.gov), ²UCLA (bmoore@ess.ucla.edu).

Introduction: The Hadean Earth is widely and enduringly pictured as a world of exuberant volcanism, exploding meteors, huge craters, infernal heat, and billowing sulfurous steams; i.e., a world of fire and brimstone punctuated with blows to the head. In the background the Moon looms gigantic in the sky. The popular image has given it a name that celebrates our mythic roots. A hot early Earth is an inevitable consequence of accretion. The Moon-forming impact ensured that Earth as we know it emerged from a fog of silicate vapor.

Much of the mantle was melted by the Moon-forming impact, and 20% was vaporized (Stevenson 1987, Canup 2004). Strong heating occurred extensively: throughout the hemisphere that was hit, everywhere in the upper mantle where impact ejecta fell back into it, and in the deep mantle because of the energy released by merging the two planet's cores. The highest temperatures are found at the surface and at the top of the core, mostly in materials that came from the impactor. If appreciable solid mantle survived the impact it's higher density suggests that it would have sunk into contact with the hot core and was melted, much as a scoop of ice cream would melt on a hot skillet.

It took only ~100 years to condense and rain out the bulk of the vaporized silicates. Water is relatively soluble in a silicate melt but other volatiles are not. To first approximation the Earth would have equilibrated with its enveloping vapors, which for most volatiles means that the Earth was substantially degassed. Relatively volatile elements may have remained present in the atmosphere throughout the magma ocean stage.

While the magma ocean was everywhere hotter than the liquidus convective cooling was extremely fast (Solomatov 2000). A crude estimate of the thermal energy available to the magma ocean is to assume that the whole mantle was on average 800 K hotter than the liquidus (roughly the difference between the condensation temperature at the cloudtops and the melting temperature at the surface), so that it contained 4×10^{30} J of readily accessible heat. To this can be added another 2×10^{30} J of easy heat in the core. Together these correspond to 20% of the impact energy.

Tidal dissipation complicates the budget by providing an energy source that is of the same order of magnitude as the thermal energy. If the Moon formed near the Roche limit, the energy dissipated raising the Moon's orbit provides another 3×10^{30} J of heating.

A magma ocean can be liquid at the surface or it can be hidden beneath a solid crust. While the surface remains mostly liquid, heat loss is determined by the thermal blanketing effect of the atmosphere. A thick CO₂-rich steam atmosphere radiates to space at the runaway greenhouse limit of ~ 300 W/m². (This is actually the asymptotic lower limit; the actual cooling rate is higher if the surface temperature exceeds 2000 K, as shown in Figure 1). A more complete estimate is that takes ~ 2 Myr to cool the magma ocean to the point where the surface freezes and the heat flow falls under the control of the mantle itself.

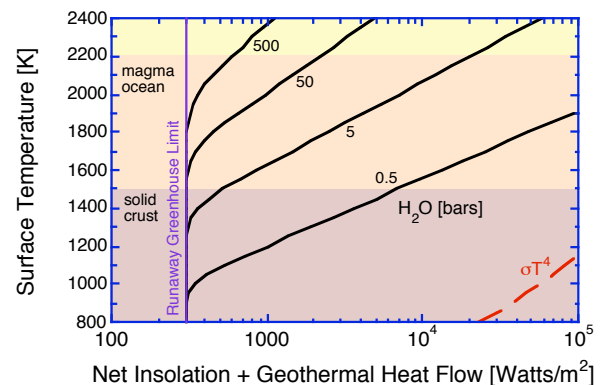


Figure 1. Radiative cooling by terrestrial steam atmospheres over a hot silicate surface. The amount of water at the surface is indicated. Also shown is the radiative cooling rate for an airless planet. Figure adapted from Abe et al 2000.

Viscous damping of tidal motions generates heat. While the mantle was molten tidal dissipation would have been relatively modest. But when and where the mantle began to freeze tidal heating would have been important. The mantle freezes from the bottom up because the melting curve is steeper than the adiabat. Consequently tidal heating was concentrated at the bottom of the mantle. The combination of tidal dissipation and atmospheric control over the heat flow created a stable governing feedback that worked through the dependence of viscosity on temperature. If tidal dissipation exceeded what the atmosphere could radiate, the excess heat raised the temperature, lowering the viscosity of the lower mantle, which in turn reduced the rate of tidal dissipation.

Evidence that things took place in this way is preserved in the lunar orbit. The lunar orbit is inclined by 5° to the ecliptic. Integrations of the lunar orbit back-

ward in time indicate that the 5° inclination to the ecliptic today maps directly into a $10\text{-}12^\circ$ inclination to Earth's equator when the Moon was near Earth (Touma and Wisdom 1994). An inclined birth-orbit is puzzling, because the giant impact origin of the Moon generates the Moon from a debris disk that revolves on the Earth's equator, and the disorderly precession of inclined orbits causes collisions that ultimately drive all the debris into orderly equatorial orbits.

Touma and Wisdom (1998) showed that the Moon could have acquired its inclination via two resonances that occur early in the evolution of the lunar orbit. The first of these occurs when lunar perigee precesses with a period of one year (the resonance is between perigee and perihelion). This resonance pumps up eccentricity. The second resonance is between the year and the combined precessions of perigee and the Moon's inclination with respect to Earth's equator. This resonance converts eccentricity into inclination.

Touma and Wisdom's mechanism works provided that the Moon's orbit evolved slowly enough that the resonances could capture it. The required rate of tidal evolution is two orders of magnitude slower than straightforward estimates of tidal dissipation rates would suggest. By controlling the rate of planetary cooling, thermal blanketing by the atmosphere slows the rate of lunar tidal evolution by three orders of magnitude. In this way the presence of a substantial steam atmosphere on Earth after the Moon-forming impact can explain the inclination of the Moon's orbit.

Water oceans condensed quickly after the mantle solidified, but for some 10-100 Myr the surface would have stayed warm (~ 500 K) until the CO_2 was removed into the mantle. How long this took is unknown, but probably not of immediate concern to this conference. Thereafter the faint young Sun suggests that a lifeless Earth would always have been evolving toward a bitterly cold ice world, but the cooling trend was frequently interrupted by volcanic or impact induced thaws.

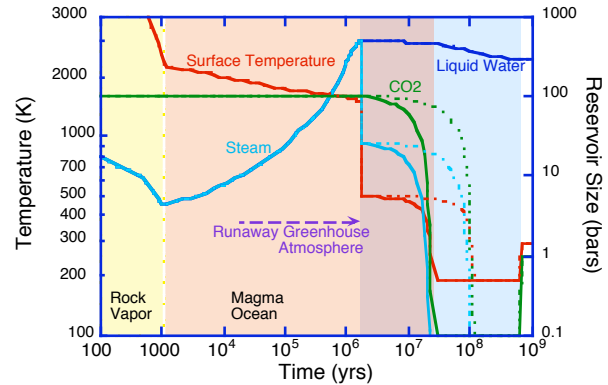


Figure 2. A cartoon history of water, temperature, and carbon dioxide in the aftermath of the moon-forming impact. How long it stays hot depends on how long it takes to scrub the CO_2 out of the atmosphere.

References:

- Canup R.M. (2004) *Icarus* 168, 433-456. Stevenson, D.J. (1987) *Ann. Rev. Earth Planet. Sci.* 15, 271--315. Solomatov V.S. (2000) In *Origin of the Earth and Moon*. R.M. Canup and K. Righter, eds. University of Arizona Press., pp. 413-433. Abe, Y., Ohtani, E., Okuchi, T., Righter, K., Drake, M. (2000) In *Origin of the Earth and Moon*. R.M. Canup and K. Righter, eds. University of Arizona Press., pp. 413-433. Touma, J., and Wisdom J. (1994) *Astron. J.* 108, 1943-1961. Touma, J., and Wisdom J. (1998) *Astron. J.* 115, 1653-1663.